IEEE Access
Multidisciplinary ⋮ Rapid Review ⋮ Open Access Journal

Received November 5, 2021, accepted November 19, 2021, date of publication November 30, 2021,
date of current version December 10, 2021.

Digital Object Identifier 10.1109/ACCESS.2021.3131518

Automated Fetal Head Classification and Segmentation Using Ultrasound Video

KHALID RASHEED[1], FARAZ JUNEJO[1], AYESHA MALIK[2], AND MUHAMMAD SAQIB[3]
[1]Faculty of Computing and Engineering Science, SZABIST, Karachi 75600, Pakistan
[2]Department of Obstetrics and Gynecology, Agha Khan University Hospital, Karachi 74800, Pakistan
[3]Faculty of Mechanical Science and Engineering, Institute of Materials Science, Technische Universität Dresden (TU Dresden), 01062 Dresden, Germany

Corresponding authors: Khalid Rasheed (khalid.rasheed@szabist.edu.pk) and Muhammad Saqib (muhammad.saqib@tu-dresden.de)

This work was supported by the Publication Fund of the TU Dresden.

ABSTRACT During pregnancy, fetal ultrasound provides essential insight into a baby's growth and development. In this ultrasound, accurate assessment of fetal head biometry is critical to the clinical management of pregnancy. Current methodologies used for fetal head biometry heavily rely upon sonographer skills and experience to locate a baby's head. In this paper a novel approach is proposed to automate the fetal head biometry using live ultrasound feed; which is also capable of tackling low abdominal contrast against surroundings. Proposed model is trained on ALEXNET and UNET for classification and segmentation of headframes respectively from ultrasound video. To compute biparietal diameter (BPD) and head circumference (HC); which are essential requirements to compute gestational age, an ellipse is drawn on the contour of the annotated segmented fetal head. It should be noted that to validate gestational age estimate, ellipse are drawn on multiple best classified headframes obtained using ALEXNET. The proposed system is able to estimate gestational age within clinically acceptable ± one week of observed gestational age with an accuracy of 96%. Moreover, it uses robust machine vision features to reduce the sonographer's interaction with the system, thus reducing the overall procedure time and making it independent of sonographer's skill.

INDEX TERMS Fetal ultrasound, fetal head biometry, head classification and segmentation, image processing, machine learning.

I. INTRODUCTION

The current process of fetal ultrasound requires sonographers to locate the fetal organs such as the head, abdomen, and femur by examining the video feed while moving the probe [1]–[3]. The slightest movement in the probe results in a drastic change in the appearance of an organ's image, while the noise produced in the video feed also hinders locating the organ [4]. Consequently, the resultant error in fetal biometry and time required are inconsistent, which may vary over the period as the sonographer gains experience [5]–[7].

Furthermore, continuous movement of the probe may irritate the mother that can lead to undesirable movement, which in turn, enhances the resultant error [8]. It should also be noted that the availability of skilled sonographers poses a great challenge [9], [10]. Consistency in ultrasound (US) measurement during the second and third trimester is of paramount importance as any error in measurement may result in inaccurate prediction with regards to fetus health [11]–[15].

For example, an 8mm error in HC causes a one-week error in gestational age estimation in the second trimester. While, in the third trimester, a 5mm error in HC causes a one-week error in gestational age. Reference [16] importantly, this error leads to the wrong Estimated Delivery Date (EDD) that increases the risk for mother and child health [17]–[19].

Head circumference (HC) and biparietal diameter (BPD), shown in Figure 1; are essential biometry parameters to estimate fetal gestational age (GA) [20], [21]. In the recent past, several systems have been proposed to automatically calculate fetal HC and BPD [22]–[31]. Lu *et al.* used randomized hough transform and K-mean algorithms to automate the measurements of BPD and HC [32]. Furthermore, McManigle applied a novel approach of boundary fragment model using random forest (RF) edge classification to automate segmentation and estimation of HC ellipse [33]. Similarly, Li *et al.* used RF with Ellipse fitting method and developed a learning-based framework that used prior knowledge of gestational age (GA) and ultrasound

The associate editor coordinating the review of this manuscript and approving it for publication was Mostafa M. Fouda.

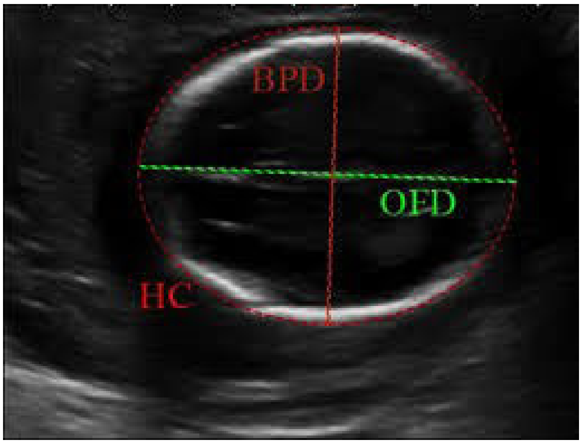

FIGURE 1. **Fetal head ultrasound shows HC, BPD and OFD.**

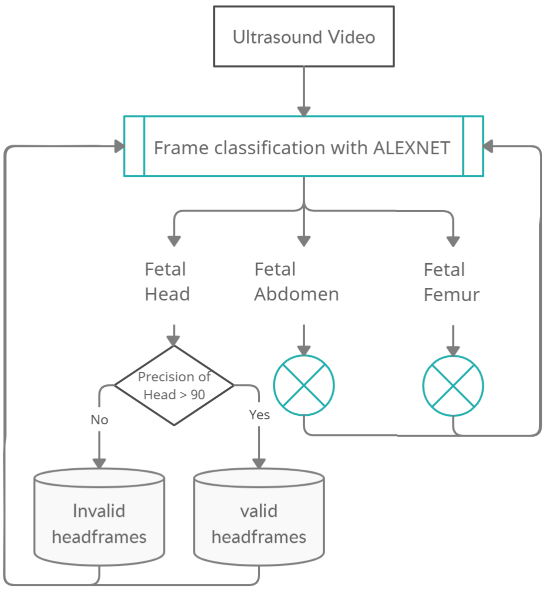

FIGURE 2. **Ultrasound video frame classification.**

scanning [23]. Ciurte *et al.* proposed a framework based on semisupervised segmentation and minimum cut problem to help in formulating fetal head segmentation and tumors detection [34]. Moreover, in addition to Hough Transform Foi *et al.* [35] and Heuval *et al.* [36] have used the Global multiscale and multi-start Nelder-Mead algorithm, respectively, with dynamic programming, to automate and detect fetal head based on 2D images. With dynamic programming to automate and detect fetal head based on 2D images.

Recently, some studies have been performed to enhance the accuracy of fetal measurements examinations. For instance, Rahayu *et al.* [37] have used a Gaussian Filter, Morphology Operation and Canny Edge Detection to reduce noises and enhance the scanning results for accurate fetal measurements. Similarly, Kirthana *et al.* [38] have used a deep-learning-based methodology named UNET with Hough transformation to improve the process of head segmentation.

Despite the advancements in fetal biometry automation, accuracy and reliability of these proposed approaches highly depend on sonographer skills, as input images are hand-picked by the sonographer, which results in very limited the sample size for any given fetus. It is therefore desirable to have an automated ultrasound measurement, i.e., making the procedure independent of the skill and experience of the sonographer.

This study presents a robust automated fetal gestational age estimation technique using live ultrasound feed. The process starts from classifying headframes using ALEXNET obtained from the video instead of the image captured by a sonographer. Furthermore, occipitofrontal diameter (OFD) measurement, shown in Figure 1, is used to validate classified headframes.

Subsequently, segmentation on head classified frames is performed by a UNET with mask and annotated images, and then Least Square Ellipse (LSE) is employed to get the HC and BPD measurements. These measurements, in turn, are used by Hadlock formula [39] to compute the fetus's gestational age (GA).

A. PROBLEM STATEMENT

Standard practice to measure fetal biometry by a sonographer or a doctor is to take images and measure linear contour and ellipsoid diameter on screen as required by American Institute for Ultrasound in Medicine (AIUM). All measurements are taken manually by the physician or sonographer; this requires both knowledge and experience. Ultrasound images are produced from sound waves, full of obnoxious noises [40], such as Gaussian noise, Poisson noise, and atmospheric absorption and scattering [41]. Owing to these noises, identifying organs becomes difficult and time-consuming for examiners [42], [43]. Furthermore, manual measurements are usually inconsistent [44] and require substantial experience [23] for repeatability. Furthermore, continued keystrokes during image acquisition may cause muscle injury to the examiner [39], [45].

There is a shortage of trained sonographers, especially in developing countries [46], [47]. This situation warrants a tremendous demand for an automated fetal biometry system. This the study employs clinically applicable automated classification, detection, localization, segmentation for fetal head biometry using ultrasound video to estimate (GA).

II. METHODOLOGY

This research proposes an approach to automate the fetal head biometry in real-time rather than on static images as employed by [22]–[31], [34]. Initially, the system auto-detects i.e., classifies frames of interest to measure fetal head biometry from an ultrasound video as shown in Figure 2. For this purpose, multiple ultrasound videos of fully developed singleton fetuses, i.e., during second and third trimesters; have been used courtesy of Agha Khan Hospital, Karachi.

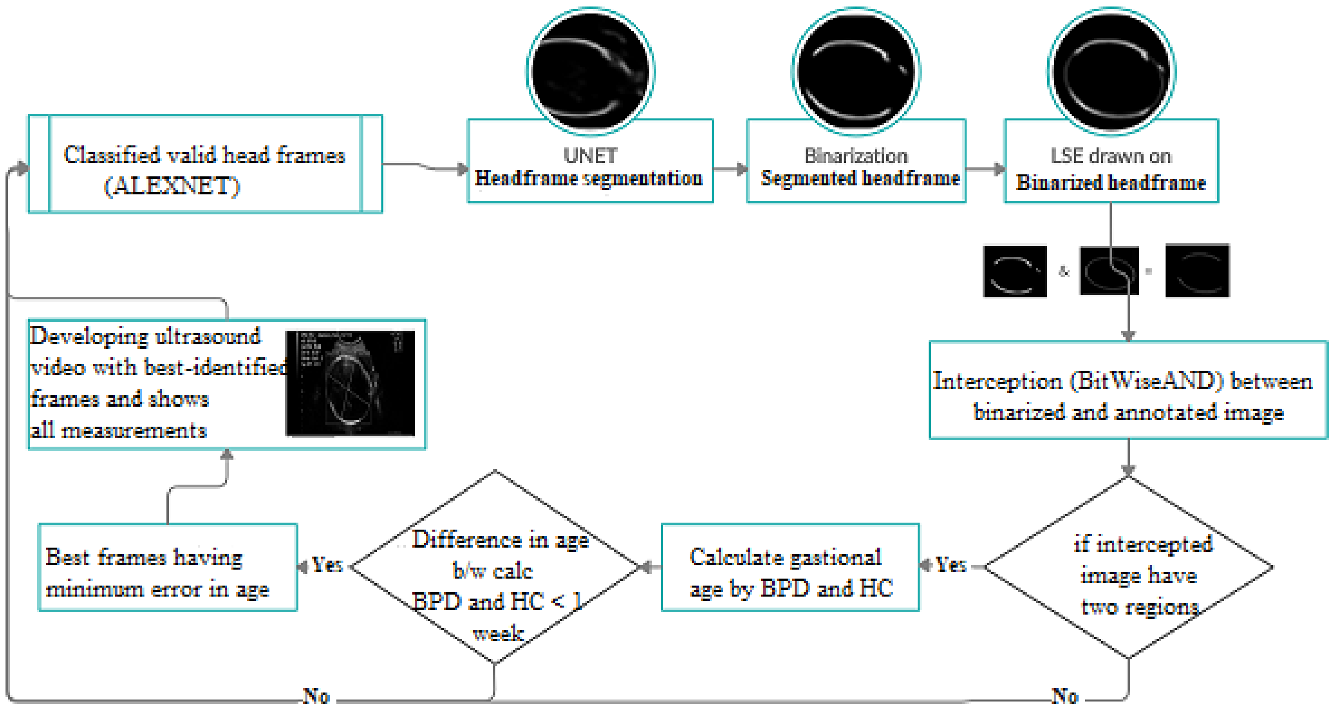

FIGURE 3. Summarized view of the proposed methodology.

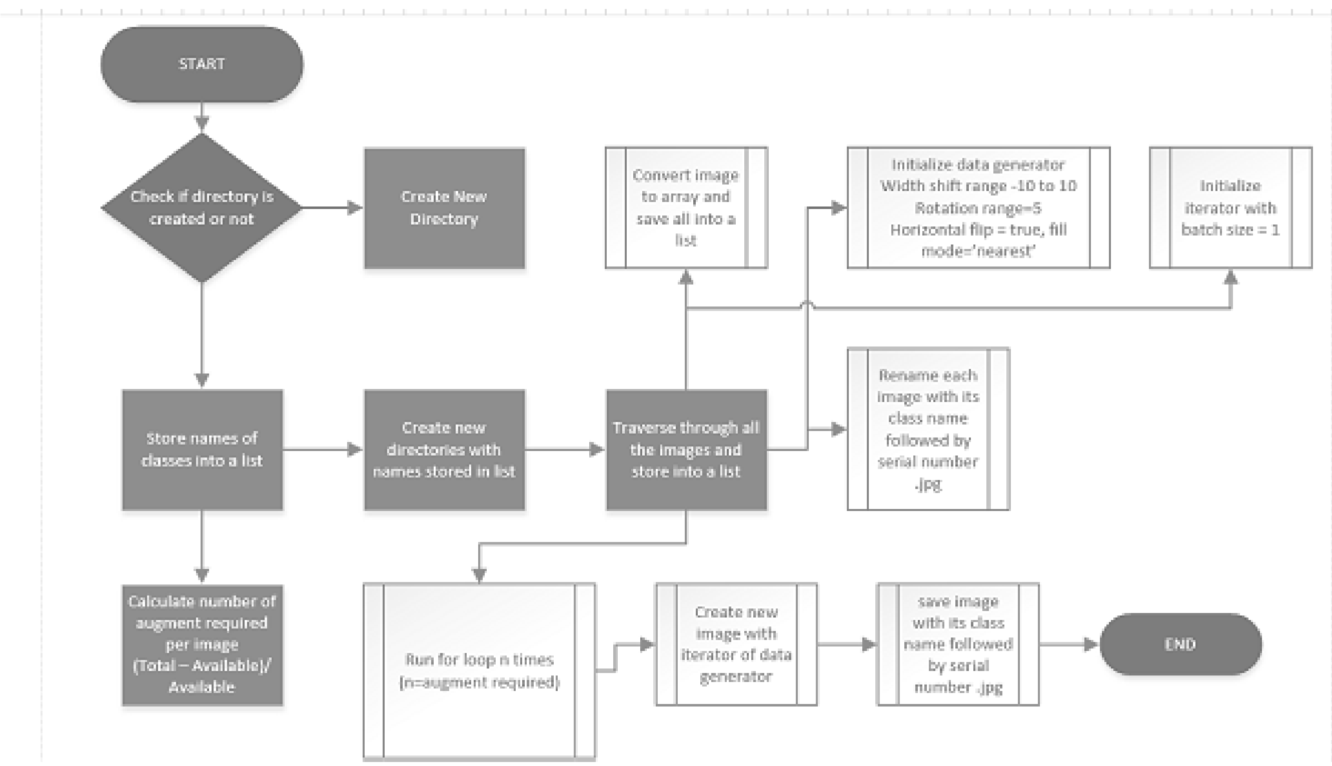

FIGURE 4. Process flow used for data augmentation.

Once the fetal head has been extracted from ultrasound video, then segmentation (as shown in Figure 3) is performed to obtain parameters i.e., BPD and HC; required for fetal Gestational age estimation.

A. DATASET CONSISTENCY

This study utilizes two different datasets; provided by AKUH. The first of these datasets contain 10,000 labeled images of each class, i.e., fetal head, femur, and abdomen. For fetal

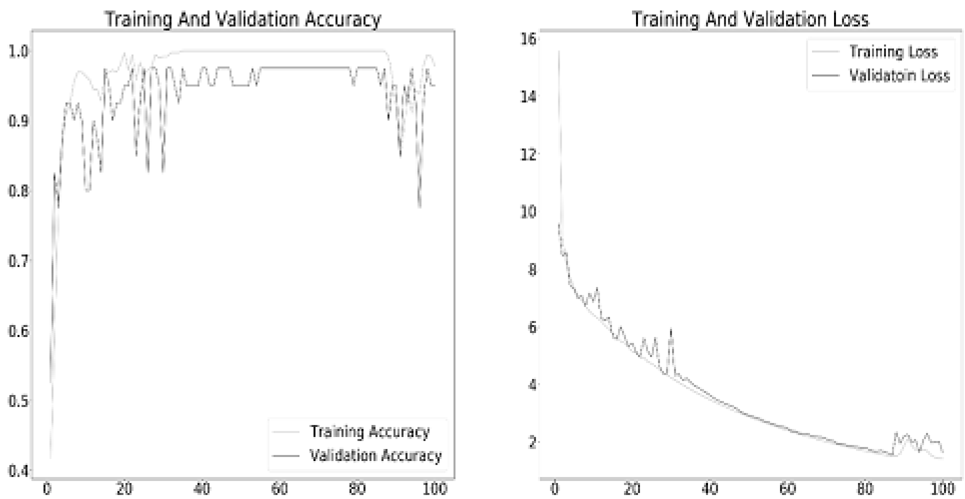

FIGURE 5. Training & validation accuracy and loss of ALEXNET.

FIGURE 6. Classified head frame using ALEXNET.

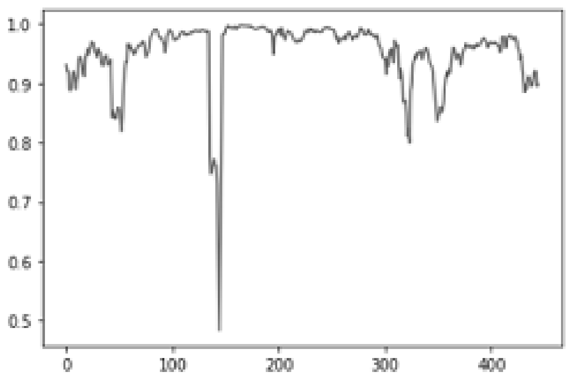

FIGURE 7. Accuracy evaluation of ALEXNET model on ultrasound video.

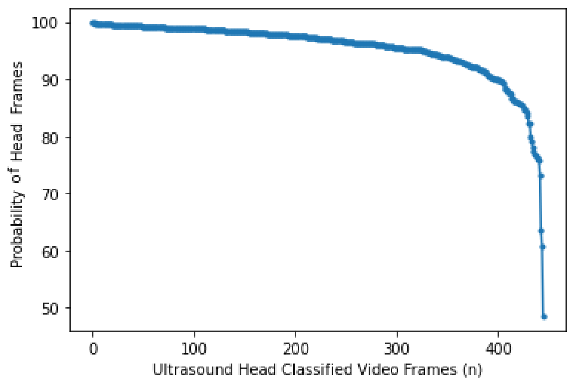

FIGURE 8. Identification of threshold value using ALEXNET results.

head biometry such as HC, BPD, and Gestational age (GA) specified by the sonographer. These images used to train ALEXNET for classification purposes. A second Dataset consisted of 1,000 ultrasound videos (DICOM Files) validated to validate the proposed model. Each tape contained all three classes, i.e., fetal head, femur, and abdomen.

B. INCLUSION & EXCLUSION CRITERIA

Inclusion criterion were:

- Maternal age between 18 and 45 years old;
- Planned delivery at AKUH; with Body mass index at first official prenatal appointment below 35.0 kg/m^2;
- Only fetal ultrasound of second and third trimester with gestational age between 18 and 42 weeks; and
- A singleton pregnancy where external fetus body fully developed to measure (abdomen, femur, and head).

Exclusion criterion were:

- Suspected fetal growth restriction or malformation of the head;
- Obesity; as it make it difficult to visualize fetal structures;
- Oligohydramnios; determined by amniotic fluid index less than 5cm; and
- Fetal distress or unstable maternal condition.

C. CLASSIFICATION

ALEXNET was used to classify, i.e., extract fetal head from ultrasound videos, which in addition to fetal head contains

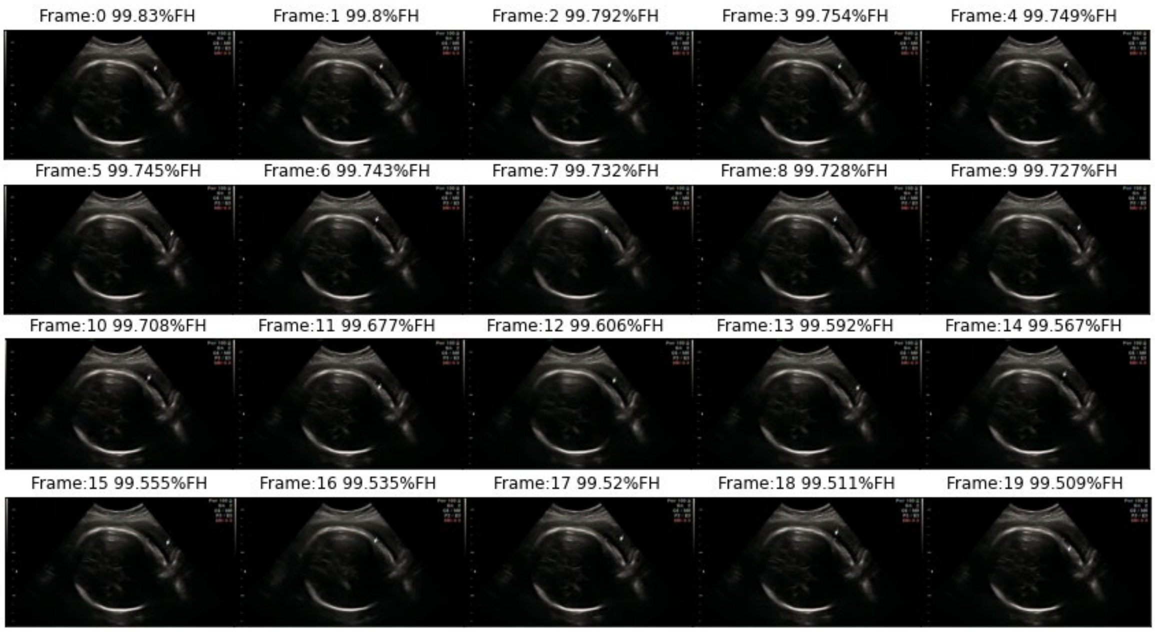

FIGURE 9. Example of best classified head frames with respective probability (% FH) obtained using ALEXNET.

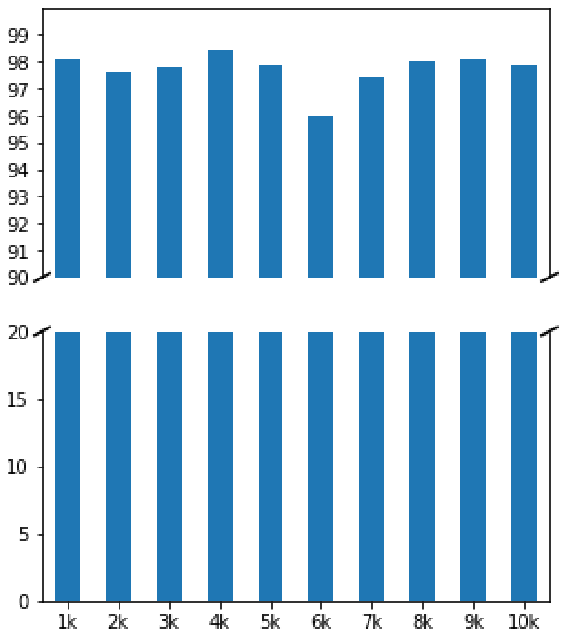

FIGURE 10. Accuracy of UNET model trained on randomly selected fetal head images.

abdomen and femur. For this purpose, training and testing of ALEXNET were performed using 10,000 static images of each class, i.e., fetal head, abdomen, and femur. Furthermore, augmentation was performed to increase the data size and simulate various organs orientations in ultrasound videos. Figure 4 enlists steps taken for data augmentation.

TABLE 1. Classification scores for the ALEXNET architecture.

	precision	recall	f1-score	support
Abdomen	0.912	0.515	0.658	200
Femur	0.894	0.715	0.794	200
Head	0.581	0.950	0.721	200
Accuracy			0.727	600
Macro Avg.	0.795	0.727	0.725	600
Weighted Avg.	0.795	0.727	0.725	600

Classification score of ALEXNET architecture are shown in Table 1.

Whereas, Figure 5 depicts accuracy and loss of training and validation of ALEXNET.

After successful training of ALEXNET, the model is evaluated on a video that contains all three classes, i.e., the fetal head, abdomen, and femur. Figure 6 shows ultrasound head classified video with a speed of 60 frames per second. The ultrasound video clip containing the head is approximately eight seconds in length, with approximately 480 frames.

Figure 7 depicts ALEXNET accuracy in extracting fetal head, which in turn is used to obtain threshold value. This threshold value is then used to identify the best fetal head frames as shown in Figure 8 from the video; which contains all frames. After extensive trials and in consultation with gynecologist; this threshold value has been identified as 90% i.e., for fetal head biometry, only those frames used which are given a score of 90 or above by ALEXNET.

Figure 9 shows some of the best head classified frames obtained using ALEXNET.

TABLE 2. Trained 12 UNET model and accuracy.

S. No.	Image Resized	Model	Additional Layers	Activation Function	Training Dataset	Accuracy
1	YES	UNET	NIL	ReLU	Mask Images	0.9844
2	YES	UNET	NIL	ELU	Mask Images	0.9824
3	YES	UNET	NIL	ReLU	Annotated Images	0.9766
4	YES	UNET	NIL	ELU	Annotated Images	0.9768
5	YES	UNET	1 Conv Layer, 1 Transpose Layer	ReLU	Mask Images	0.9831
6	YES	UNET	1 Conv Layer, 1 Transpose Layer	ELU	Mask Images	0.9817
7	YES	UNET	1 Conv Layer, 1 Transpose Layer	ReLU	Annotated Images	0.9782
8	YES	UNET	1 Conv Layer, 1 Transpose Layer	ELU	Annotated Images	0.9703
9	YES	UNET	2 Conv Layer, 2 Transpose Layer	ReLU	Mask Images	0.8463
10	YES	UNET	2 Conv Layer, 2 Transpose Layer	ELU	Mask Images	0.7359
11	YES	UNET	2 Conv Layer, 2 Transpose Layer	ReLU	Annotated Images	0.9775
12	YES	UNET	2 Conv Layer, 2 Transpose Layer	ELU	Annotated Images	0.9687

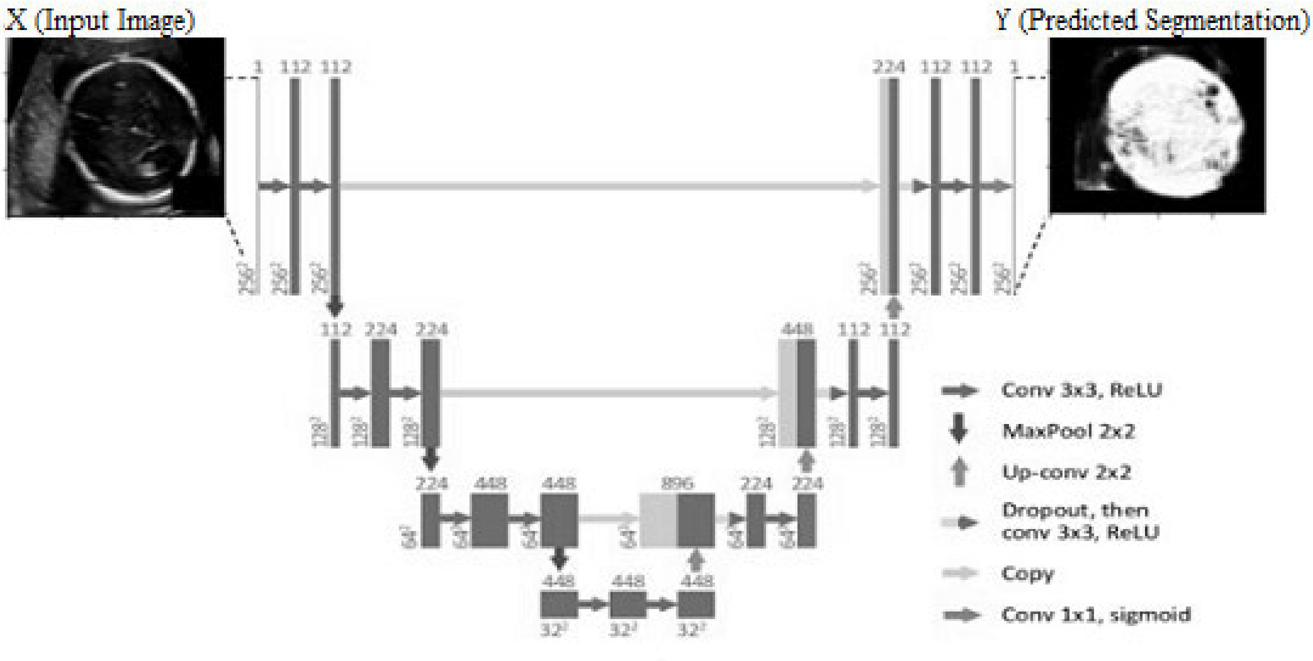

FIGURE 11. Localization and segmentation with UNET (mask approach).

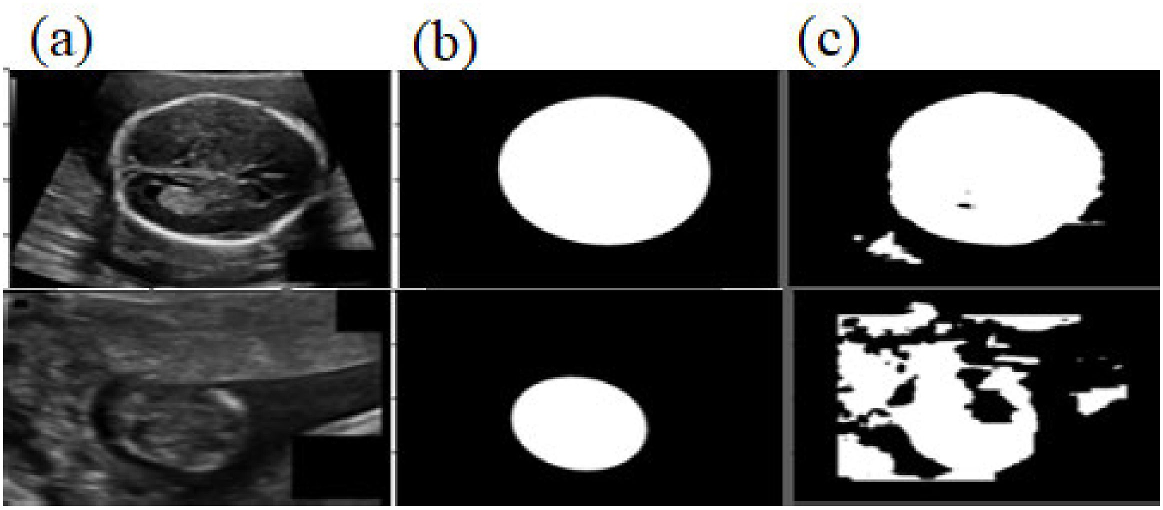

FIGURE 12. UNET-head mask prediction results: (a) input fetal head image, (b) ground truth, and (c) output predicted image using UNET mask approach.

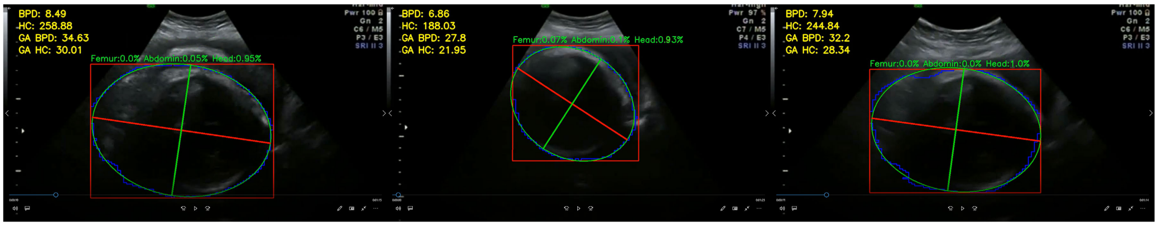

FIGURE 13. Sample frame of video output for localization segmentation and measurement.

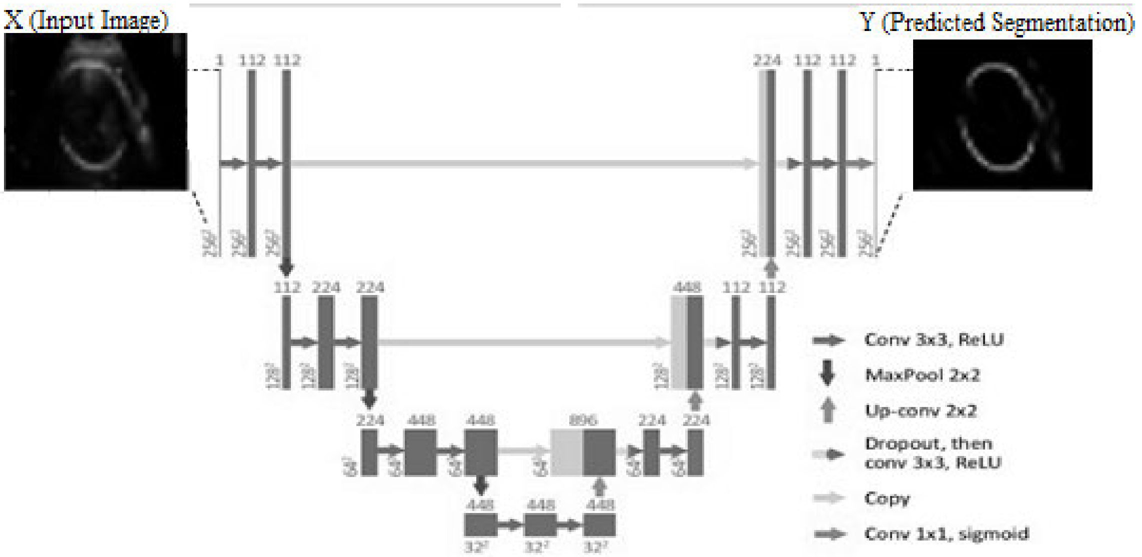

FIGURE 14. Localization and segmentation with UNET (Annotated approach).

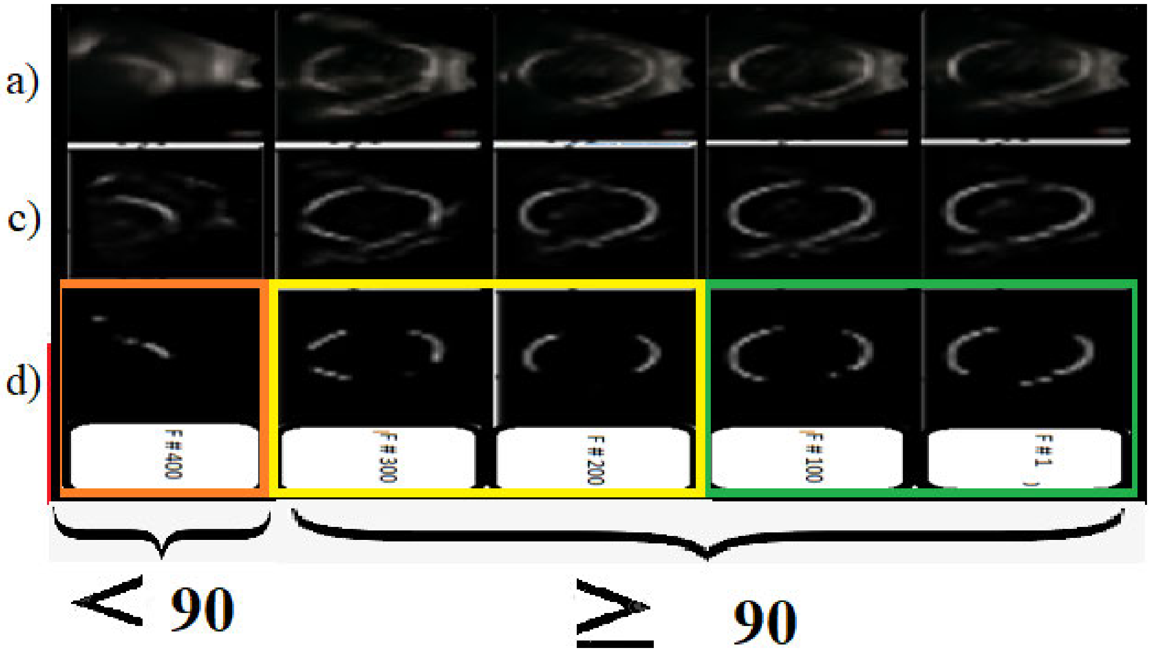

FIGURE 15. Taking best-classified frame: a) shows head classified frame, b) segmentation using UNET of classified head frames, and c) thresholding on segmentation.

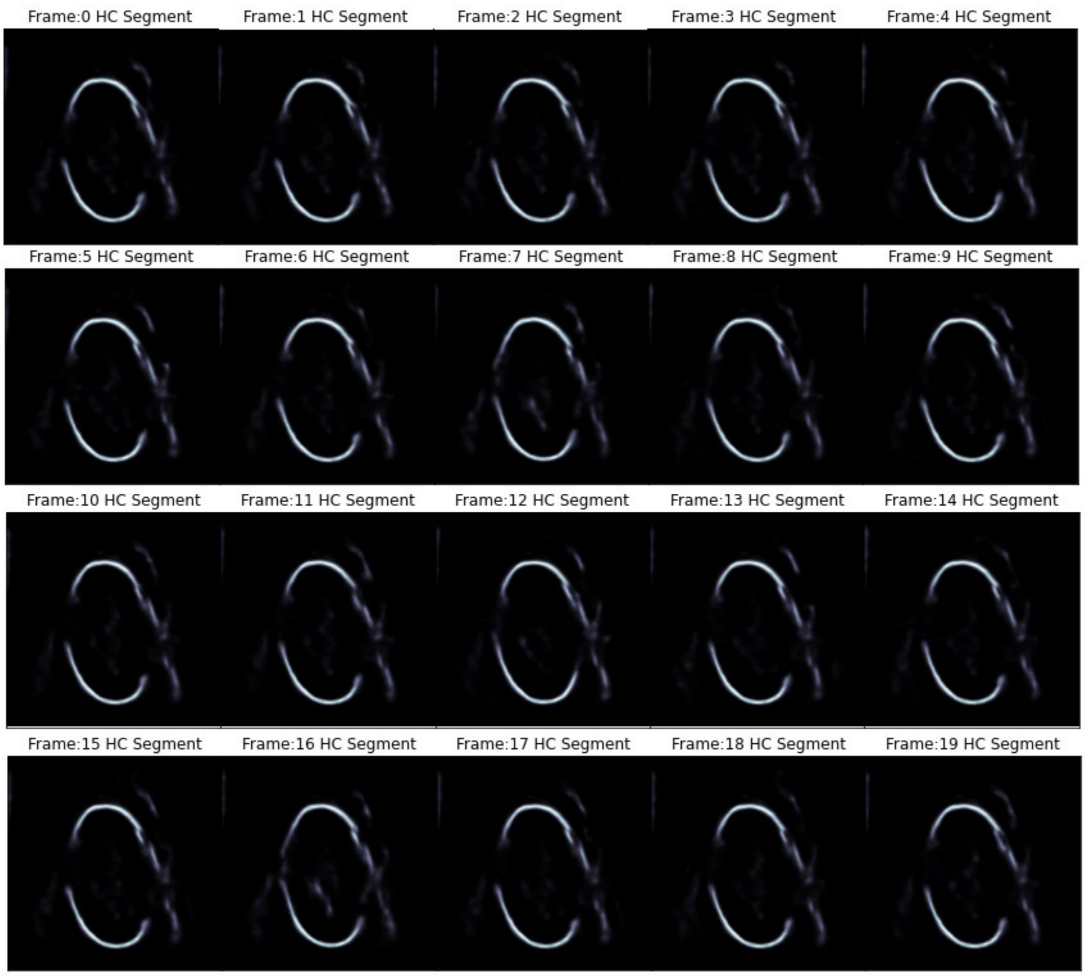

FIGURE 16. Segmentation on all best classified fetal head frames of ultrasound video with annotated UNET model.

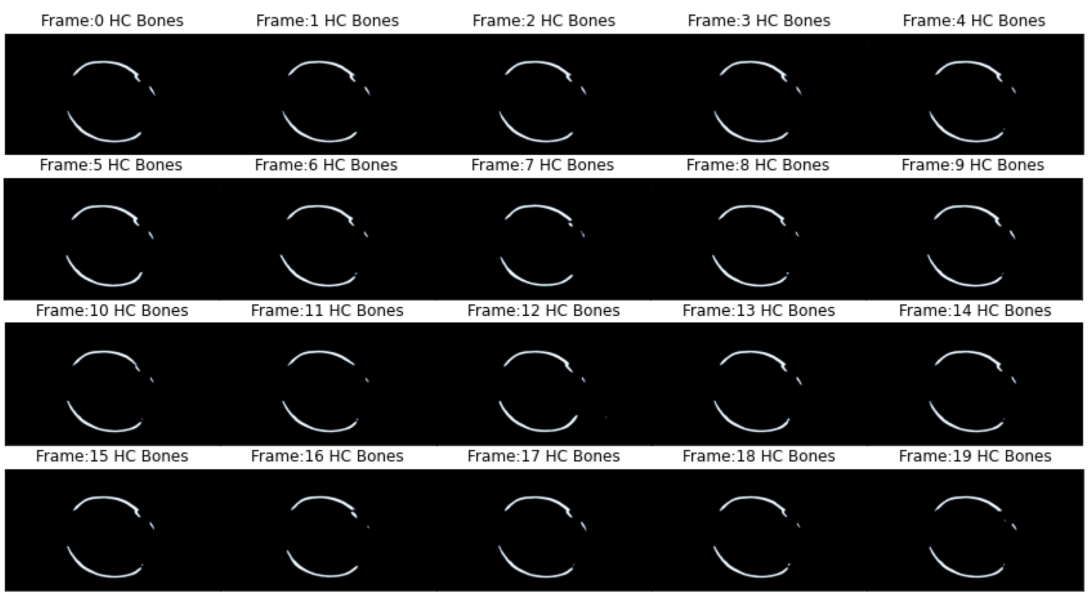

FIGURE 17. Binarization of segmented frames.

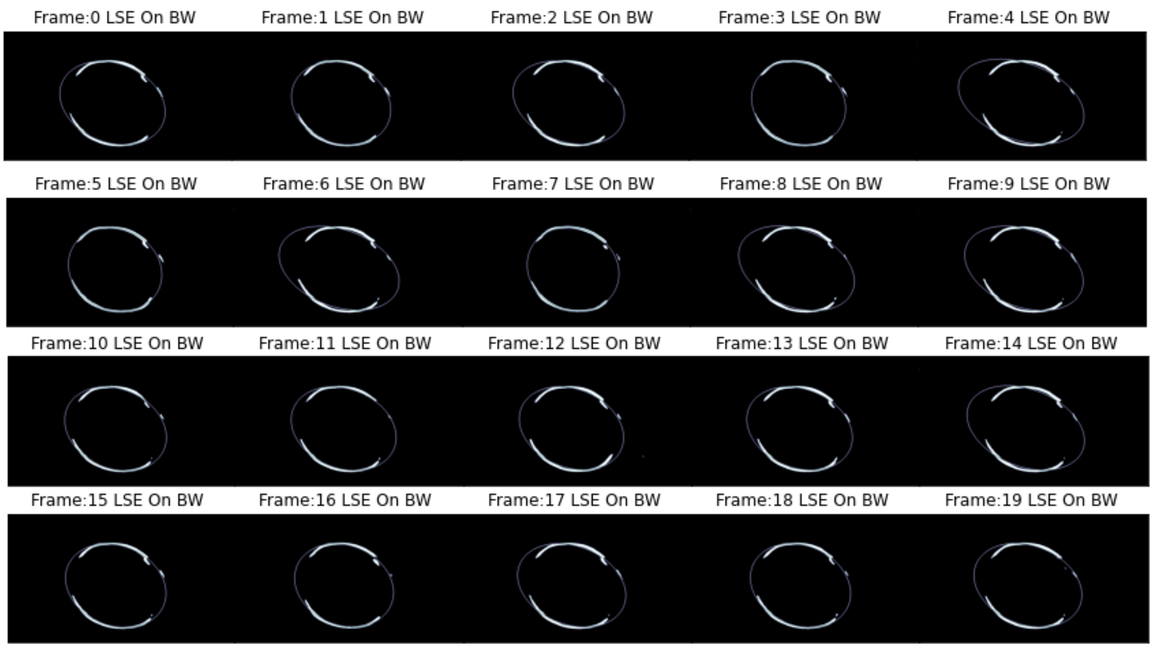

FIGURE 18. **Least square ellipse method to draw an ellipse on the contour of binarized frames.**

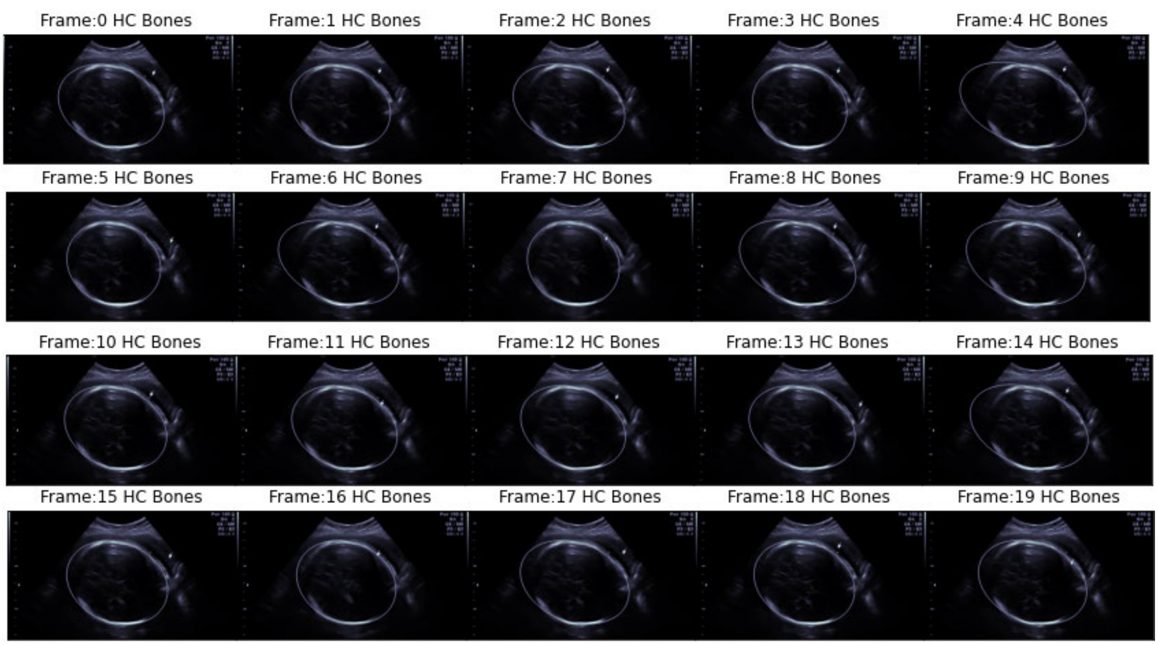

FIGURE 19. **Calculated ellipses on actual frame.**

1) SEGMENTATION

Upon completion of classification, all valid head frames are used to produce a video containing fetal head only. A single frame of such video is shown in Figure 6, which enlist the probability of each organ and frame number. This video is then used for head segmentation and biometry purposes.

For segmentation purposes, For segmentation purposes, UNET model is trained with 10,000 labeled fetal head images. From this dataset, UNET model has been trained on 1,000, 2,000, 3,000 and on up to 10,000 images, which were selected randomly. Figure 10 shows the accuracy of model for these datasets.

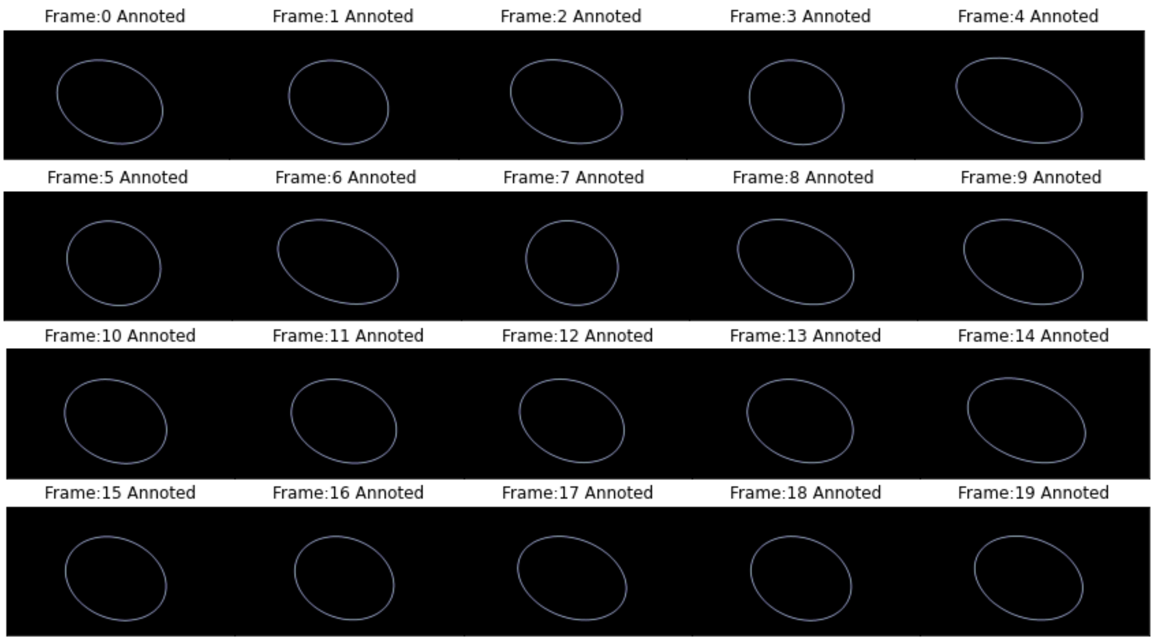

FIGURE 20. Annotation on best classified head frames.

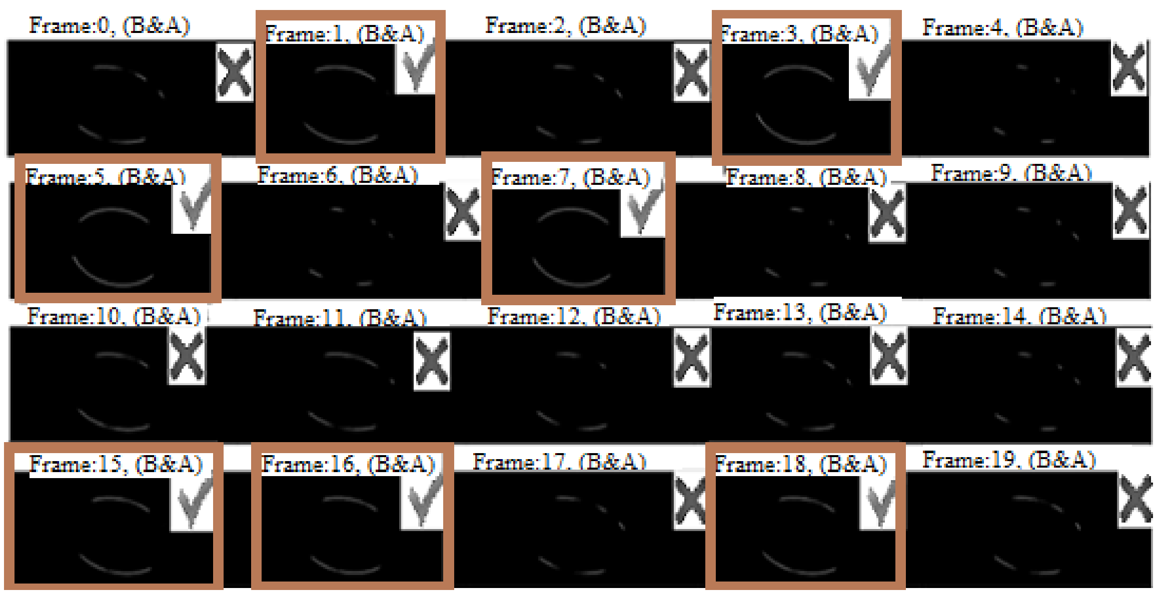

FIGURE 21. Bitwise AND between threshold segmented and annotated images of head classified frames of ultrasound video.

It is evident from Figure 10 that increase in size of dataset does not increase the accuracy of the system drastically. This is primarily due to the fact that ultrasound head images used for this study are of second and third trimesters; by which time Biparietal bones, used for fetal head biometry are quite visible.

Subsequently, UNET model is trained with different variations; enlisted in Table 2 using both masked and annotated approaches. Results show that highest accuracy obtained using mask and annotated approach are 98.44% and 97.82% respectively; and increase of convolve and transpose layers to UNET architecture does not improve results.

Figure 11 shows result of best performing UNET configuration model (selected from Table 2) with mask approach.

However, during validation (some results shown in Figure 12, it was determined that sometimes a complete ellipse is not found using mask approach, which is an essential requirement for fetal head biometry.

After training of UNET model with mask; localization and segmentation are performed on all classified head frames.

TABLE 3. **Measurement of calculated and observed BPD, HC, OFD and gestational age using BPD and HC approach on best-classified head frames from ultrasound video of 36th week gestational age.**

BI	Obs BPD	Calc BPD	BPD Error	Obs OFD	Calc OFD	OFD Error	Obs HC	Calc HC	HC Error	Obs Age	Calc Age BPD	Calc Age HC
5	88	85.220	2.780	112	117.920	-5.920	312	323.200	-11.200	36W0D	34W5D	37W2D
2	88	86.740	1.260	112	110.360	1.640	312	311.820	0.180	36W0D	35W3D	36W1D
5	88	84.370	3.630	112	124.640	-12.640	312	334.350	-22.350	36W0D	34W3D	38W3D
2	88	88.100	-0.100	112	104.460	7.540	312	303.560	8.440	36W0D	36W1D	35W2D
5	88	82.620	5.380	112	141.730	-29.730	312	364.430	-52.430	36W0D	33W4D	41W2D
2	88	88.100	-0.100	112	103.750	8.250	312	302.360	9.640	36W0D	36W1D	35W1D
5	88	82.900	5.100	112	135.170	-23.170	312	352.250	-40.250	36W0D	33W5D	40W1D
2	88	88.380	-0.380	112	101.790	10.210	312	299.460	12.540	36W0D	36W2D	34W5D
5	88	83.200	4.800	112	131.060	-19.060	312	344.850	-32.850	36W0D	33W6D	39W4D
5	88	83.050	4.950	112	133.850	-21.850	312	349.930	-37.930	36W0D	33W6D	39W7D
3	88	85.620	2.380	112	114.150	-2.150	312	316.980	-4.980	36W0D	34W7D	36W5D
4	88	85.620	2.380	112	117.420	-5.420	312	322.820	-10.820	36W0D	34W7D	37W2D
4	88	84.440	3.560	112	117.140	-5.140	312	320.780	-8.780	36W0D	34W3D	37W1D
5	88	84.890	3.110	112	118.250	-6.250	312	323.370	-11.370	36W0D	34W4D	37W3D
5	88	83.240	4.760	112	132.570	-20.570	312	347.740	-35.740	36W0D	33W6D	39W5D
2	88	86.130	1.870	112	112.250	-0.250	312	314.300	-2.300	36W0D	35W1D	36W3D
2	88	86	2	112	110.320	1.680	312	310.740	1.260	36W0D	35W1D	36W0D
5	88	84.530	3.470	112	121.510	-9.510	312	328.820	-16.820	36W0D	34W3D	37W7D
2	88	86.020	1.980	112	112.270	-0.270	312	314.190	-2.190	36W0D	35W1D	36W3D

Where;

- BI: Number of objects identified during interception
- Obs BPD, Obs HC & Obs Age : BPD, HC and Gestational age observed by sonographer
- Calc BPD, Calc HC & Calc Age: Calculated BPD, HC and Gestational age using proposed approach

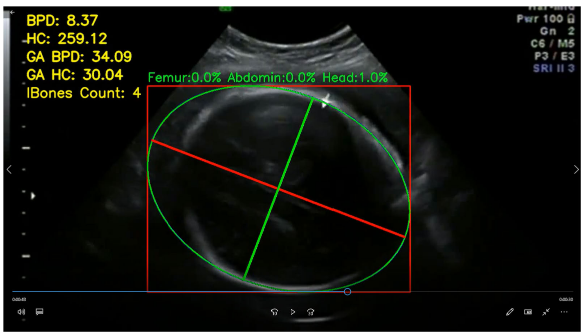

FIGURE 22. **US video frames with estimation of head circumference using least square ellipse.**

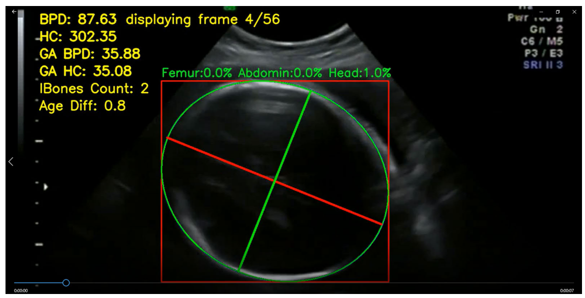

FIGURE 23. **US video frames with estimation of head circumference using LSE for only frames having bones after Bitwise AND of annotated and thresholded images of ultrasound best-classified frames.**

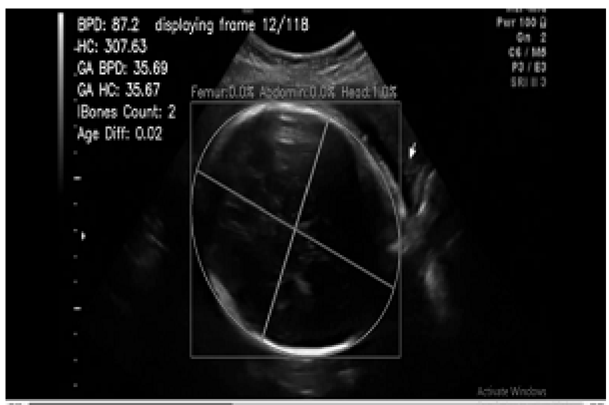

FIGURE 24. **US video summarizes the view of all steps taken to select the best frames.**

To obtain a perfect ellipse depicting fetal head, Least Square Ellipse [50]–[52] approach is used on the contour of the predicted mask. It can be seen from Figure 13, that resultant ellipse is not a true representation of fetal head.

Training of UNET model with mask approach was therefore abandoned instead annotated approach was used as shown in Figure 14.

Furthermore, Figure 15 shows results for different precisions of head class obtained using ALEXNET. As discussed earlier; only frames with precision higher than a threshold of 90 % or more are used for segmentation purposes.

It can be seen from Figure 16 that better segmentation results i.e. Biparietal bones are clearly visible; are obtained for valid head frames (threshold $> 90\%$) obtained using ALEXNET. However, presence of noises imply that Binarization must be applied.

The primary objective of this study is to identify the best frame on which fetal biometry can be performed. It should be noted that a sonographer spends a significant amount of time ascertaining the best frames for repeated measurements [53]. To measure fetal head circumference, initially,

TABLE 4. Measurement of calculated and observed gestational age using BPD and HC approach with difference in age on best-classified head sample frame from ultrasound video of 36th week gestational age.

	BI	Obs Age	Calc Age Using BPD	Calc Age Using HC	Diff
Frame 0 with prec 0.9983	5	36W0D	34W5D	37W2D	2W4D
Frame 1 with prec 0.998	2	36W0D	35W3D	36W1D	0W5D
Frame 2 with prec 0.99792	5	36W0D	34W3D	38W3D	4W1D
Frame 3 with prec 0.99752	2	36W0D	36W1D	35W2D	0W6D
Frame 4 with prec 0.99749	5	36W0D	33W4D	41W2D	7W4D
Frame 5 with prec 0.99745	2	36W0D	36W1D	35W1D	1W0D
Frame 6 with prec 0.99743	5	36W0D	33W5D	40W1D	6W3D
Frame 7 with prec 0.99732	2	36W0D	36W2D	34W5D	1W3D
Frame 8 with prec 0.99728	5	36W0D	33W6D	39W4D	5W4D
Frame 9 with prec 0.99727	5	36W0D	33W6D	39W7D	6W1D
Frame 10 with prec 0.99708	3	36W0D	34W7D	36W5D	1W5D
Frame 11 with prec 0.99677	4	36W0D	34W7D	37W2D	2W2D
Frame 12 with prec 0.99606	4	36W0D	34W3D	37W1D	2W5D
Frame 13 with prec 0.99592	5	36W0D	34W4D	37W3D	2W5D
Frame 14 with prec 0.99567	5	36W0D	33W6D	39W5D	5W6D
Frame 15 with prec 0.99555	2	36W0D	35W1D	36W3D	1W1D
Frame 16 with prec 0.99535	2	36W0D	35W1D	36W0D	0W6D
Frame 17 with prec 0.9952	5	36W0D	34W3D	37W7D	3W3D
Frame 18 with prec 0.99511	2	36W0D	35W1D	36W3D	1W2D

Where;

- BI: Number of objects identified during interception
- Obs Age : Gestational age observed by sonographer
- Calc Age: Calculated gestational age using proposed approach
- Diff: difference in age between age calculated using BPD and HC

TABLE 5. Mean gestational age between gestational age calculation using BPD and HC approach on sample frames having two objects identified during interception from ultrasound video of 36th week gestational age.

	BI	Obs Age	Calc Age Using BPD	Calc Age Using HC	Diff	Mean Age
Frame 1 with prec 0.998	2	36W0D	35W3D	36W1D	0W5D	35W6D
Frame 3 with prec 0.99752	2	36W0D	36W1D	35W2D	0W6D	35W5D
Frame 5 with prec 0.99745	2	36W0D	36W1D	35W1D	1W0D	35W4D
Frame 7 with prec 0.99732	2	36W0D	36W2D	34W5D	1W3D	35W4D
Frame 15 with prec 0.99555	2	36W0D	35W1D	36W3D	1W1D	35W6D
Frame 16 with prec 0.99535	2	36W0D	35W1D	36W0D	0W6D	35W4D
Frame 18 with prec 0.99511	2	36W0D	35W1D	36W3D	1W2D	35W5D

Where;

- BI: Number of objects identified during interception
- Obs Age : Gestational age observed by sonographer
- Calc Age: Calculated gestational age using proposed approach
- Diff: difference in age between age calculated using BPD and HC

TABLE 6. Less than one week gestational age difference between gestational age calculation using BPD and HC approach on sample frames having two objects identified during interception and from ultrasound video of 36th week gestational age.

BI	Obs Age	Calc Age Using BPD	Calc Age Using HC	Diff	Mean Age
2	36W0D	35W3D	36W1D	0W5D	35W6D
2	36W0D	36W1D	35W2D	0W6D	35W5D
2	36W0D	36W1D	35W1D	1W0D	35W4D
2	36W0D	35W1D	36W0D	0W6D	35W4D
				Proposed Age	35W5D

Where;

- BI: Number of objects identified during interception
- Obs Age :Gestational age observed by sonographer
- Calc Age: Calculated gestational age using proposed approach
- Diff: difference in age between age calculated using BPD and HC

TABLE 7. Result with performance in frame selection and fetal gestational age estimation on 2 different fetus ultrasound videos of 36 and 18 weeks.

Gender	Boy	Girl
Pixel Size	0.194	0.105
Total Frames	480	3135
Total head classified frames in ultrasound video using ALEXNET	275	2825
Total frames having two objects identified during interception	79	115
Total frames with less than one week age difference between calculated age using HC and BPD approach	27	98
Observed gestational age	36 week (s) 0 Day (s)	18 week (s) 4 Day (s)
Proposed gestational age	35 week (s) 5 Day (s)	18 week (s) 1 Day (s)

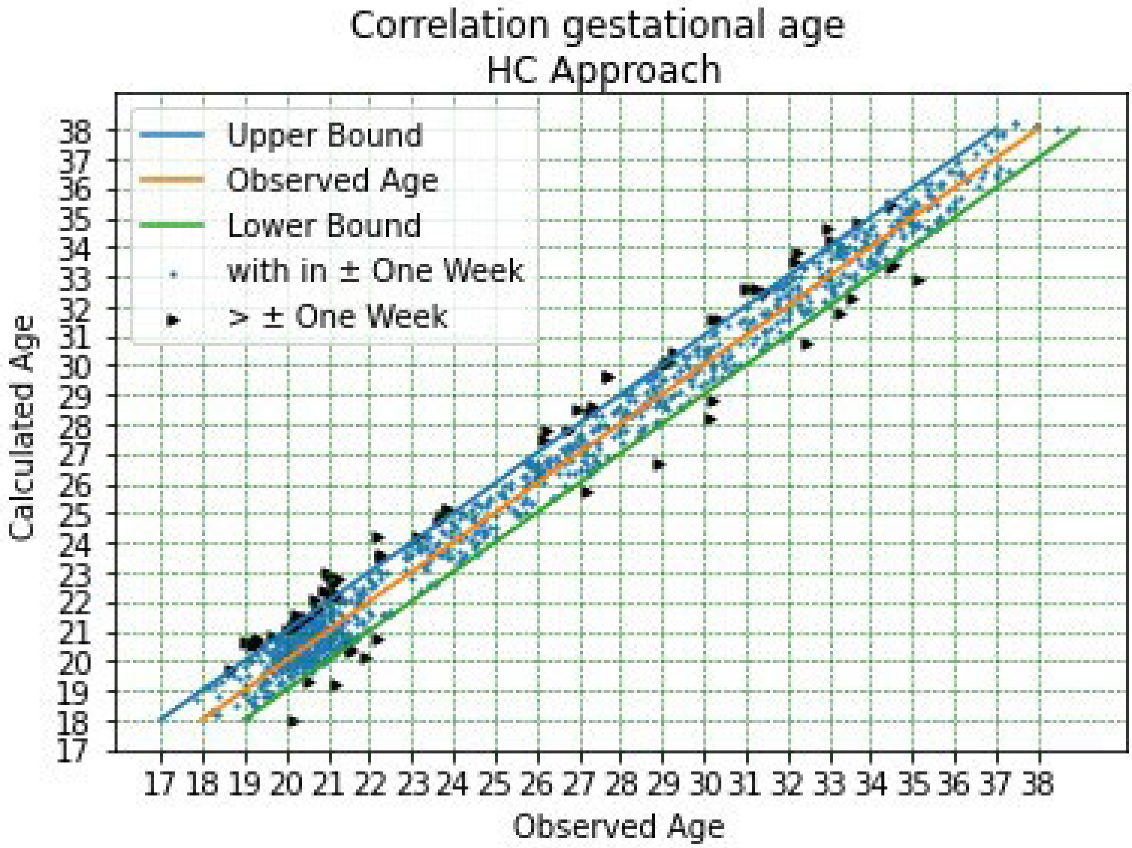

FIGURE 25. Correlation gestational age for observed and calculated using HC approach with lower and upper bound of one week.

grayscale images, shown in Figure 16 were binarize using eq(1) as shown in Figure 17.

$$g(x, y) = \begin{cases} 1 & \text{if } f(x, y) \geq T, \\ 0 & \text{otherwise} \end{cases} \quad (1)$$

where g(x, y) is a thresholded version of f(x, y) at some global threshold T,

After Binarization, it can be seen from Figure 17 that noises are removed and contour of Biparietal bones are clearly visible.

Now for drawing of an ellipse, as shown in Figure 18; Least Square Ellipse method is used. It can be seen that for some cases, i.e., Frame 0, 2, 6, 8 and 9, ellipses are not properly touching the contour of Biparietal bones.

Afterward, for validation purposes; the resultant Ellipses are superimposed on the actual frames, as shown in Figure 19.

As discussed earlier, in some cases ellipses are not properly touching contour of Biparietal bones, which results in erroneous measurement. To exclude such frames; initially for each frame an annotated image is created by superimposing respective binary ellipse on a dark image i.e. containing all pixels of 0; as shown in Figure 20. Now; interception is performed between each binarize segmented frame (shown in Figure 17) and corresponding annotated image (shown in Figure 20). This will yield only common pixels as shown in Figure 21. Based on pixel connectivity, it can be seen that for cases in which overlap occurs between ellipse and Biparietal bones, there are only two objects as shown in Figure 21. Whereas; otherwise number of objects are greater than two as shown in Figure 21. However, this interception process is quite time consuming. To overcome this problem, frames with invalid OFD are identified and discarded. For this purpose, major axis of ellipse i.e. OFD is computed for each frame. This value of OFD is then compared with specified range of OFD defined for second and third trimester [54], [55]. Now, interception is performed using eq(2) for only frames with valid OFD.

$$Ii = A_i \cap B_i \quad (2)$$

where

n = no of classified head frames from ultrasound video,
A = Binarized segmented frame
B = Annotated frame
I = Intercepted image

Fetal gestational age is then computed for all frames through two parameters i.e. HC and BPD separately using

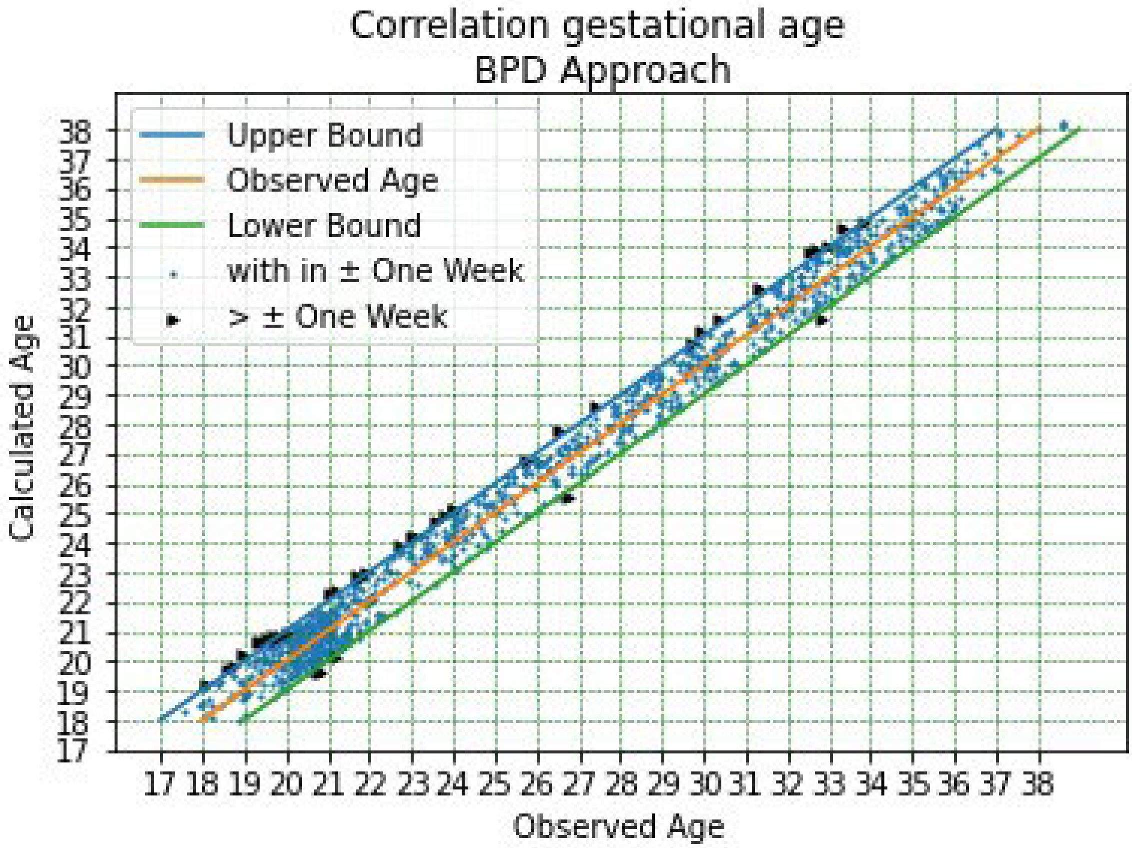

FIGURE 26. **Correlation gestational age for observed and calculated using BPD approach with lower and upper bound of one week.**

respective Headlock formulas [56], as shown in Table 3. It is evident from Table 3 that as expected frames with only two objects yield gestational age with better accuracy when compared with gestational age observed by sonographer. To compare between frames containing two objects and more than two objects; two different videos were made. One video contained all frames (shown in Figure 22) and the other video contained only frames having two objects (as shown in Figure 23).

It can be seen from these videos that as expected gestational age measured using video containing frames with only two objects is closer to gestational age observed by sonographer. However, still for such frames i.e. containing two objects only, occasionally age measured using BPD and HC are far apart as shown in Figure 23. It is also noted that age estimation using BPD is accurate in comparison to age computed using HC, it is primarily due to the fact that due to surrounding noise biparietal bones do not appear to meet each other, hence approximation is involved in computing HC. To overcome this problem, age computed using HC and BPD are compared with each other, as shown in Table 4. Afterwards, only frames for which difference in estimated age using both parameters i.e. BPD and HC is within one week of each other using eq(3,4 and 5) i.e. within allowable tolerance are shortlisted for fetal biometry as shown in Table 5. Finally, a video is made containing only shortlisted frames; as depicted in Table 6 and as shown in Figure 24. This approach implies any false positive frames are discarded prior to gestational age measurement.

$$Ci = |Ai - Bi| \quad i = 1, 2, 3, 4, \ldots\ldots n \tag{3}$$

$$\begin{cases} mj = \dfrac{Ai + Bi}{2} & \text{if } Ci \leq 1, \\ dontconsider & \text{otherwise} \end{cases} \tag{4}$$

$$M = \frac{1}{j}\sum_{k=1}^{j} mk \tag{5}$$

where

n = no of classified head frames from ultrasound video,
j = no of frames having Age Diff <= 1
A = Calculated Age Using BPD Approach
B = Calculated Age Using HC Approach
M = Proposed Age

As discussed, ultrasound video of 36$\hat{t}$h week gestational age is used; all figures are shown for pre-processing and post-process of model classification, and segmentation are used to

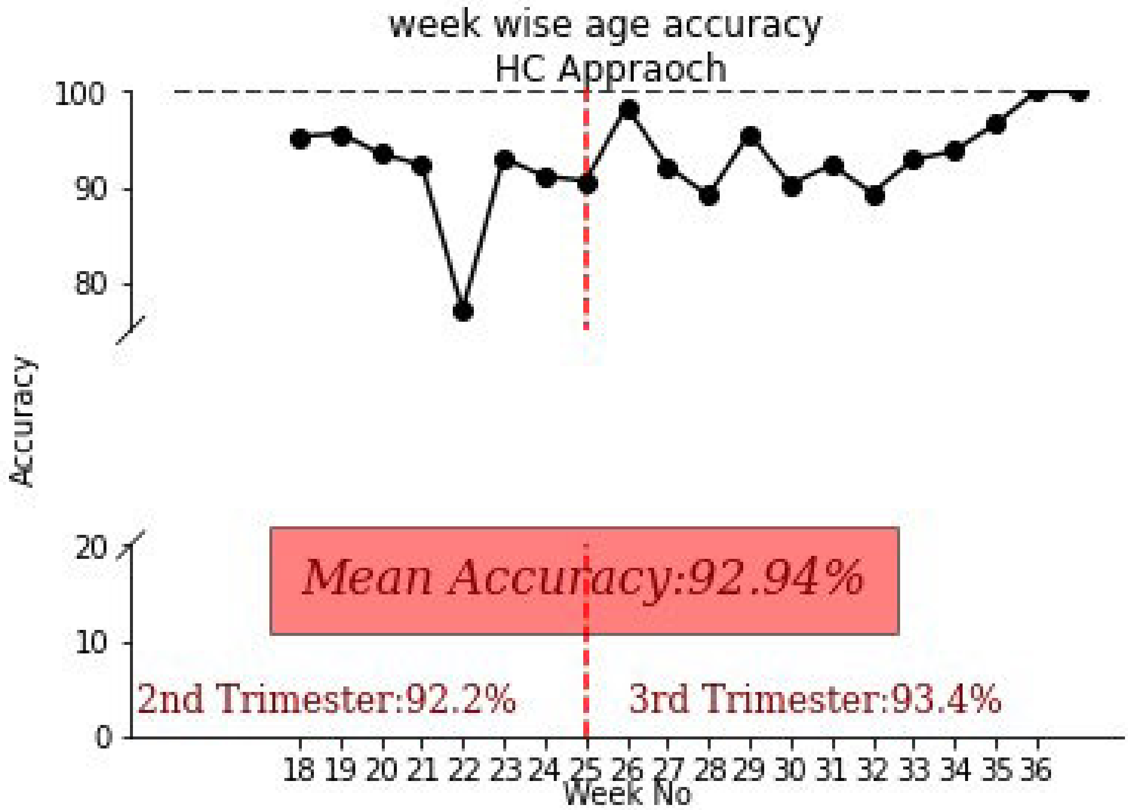

FIGURE 27. **Week wise gestational age accuracy with HC approach and breakdown with semester wise.**

show frames of a sample video. Then, all steps are combined to produce an ultrasound video clip containing the fetal head of 36t̂h week gestational age with approximately 480 frames, having a speed of 60 frames per second. Finally, the result is obtained as mentioned in Table 7 with 27 frames selected in the ultrasound video clip. Each frame is classified with a fetal head frame. Besides, a system proposed in this study produces only 27 frames, and all frames give a result with a minimum error on the estimation of fetal gestational age as shown in Figure 24.

III. RESULTS AND DISCUSSION

A total of 1000 ultrasound videos of the second and the third trimesters (range: 18 to 40 weeks gestational age) were used to evaluate the performance of the proposed system in predicting fetal gestational age. It should be noted that allowable tolerance is ± 1 week. For this purpose, initially, gestational age is calculated using fetal biometry parameters, i.e., HC and BPD separately, as shown in Figure 25 and Figure 26, respectively.

Comparison of calculated age with observed age for different trimesters using HC and BPD measurement, respectively; shows reasonable accuracy of 92 % - 97 % as depicted in Figure 27 and Figure 28, respectively.

It was observed that age estimation using BPD parameter provides better accuracy in comparison to that with HC parameter for both second and third trimesters as depicted in Table 8. Primarily, in few instances presence of excessive noise occurs in the region where due to the invisibility of solid tissues of the fetal head causes gaps, as shown in Figure 29; which in turn causes error in drawing the best fit ellipse. Furthermore, accuracy improves in the third trimester in comparison to the second trimester as with the progression of pregnancy organs growth implies that they appear with more the clarity in ultrasound. It can be seen that when both parameters i.e., HC and BPD are used simultaneously to calculate gestational age, accuracy improves slightly, as shown in Table 8.

It is therefore proposed to use both parameters in computing gestational age, as it results in the accuracy of 96 – 97 %. Week wise results of proposed approach are shown in Figure 30.

IV. CONCLUSION AND FUTURE WORK

The proposed system can estimate gestational age within clinically acceptable ± one week of observed gestational age with an accuracy of 96%. The system takes ten to fifteen minutes to compute fetal gestational age using fetus ultrasound video. The computation time depends on the length

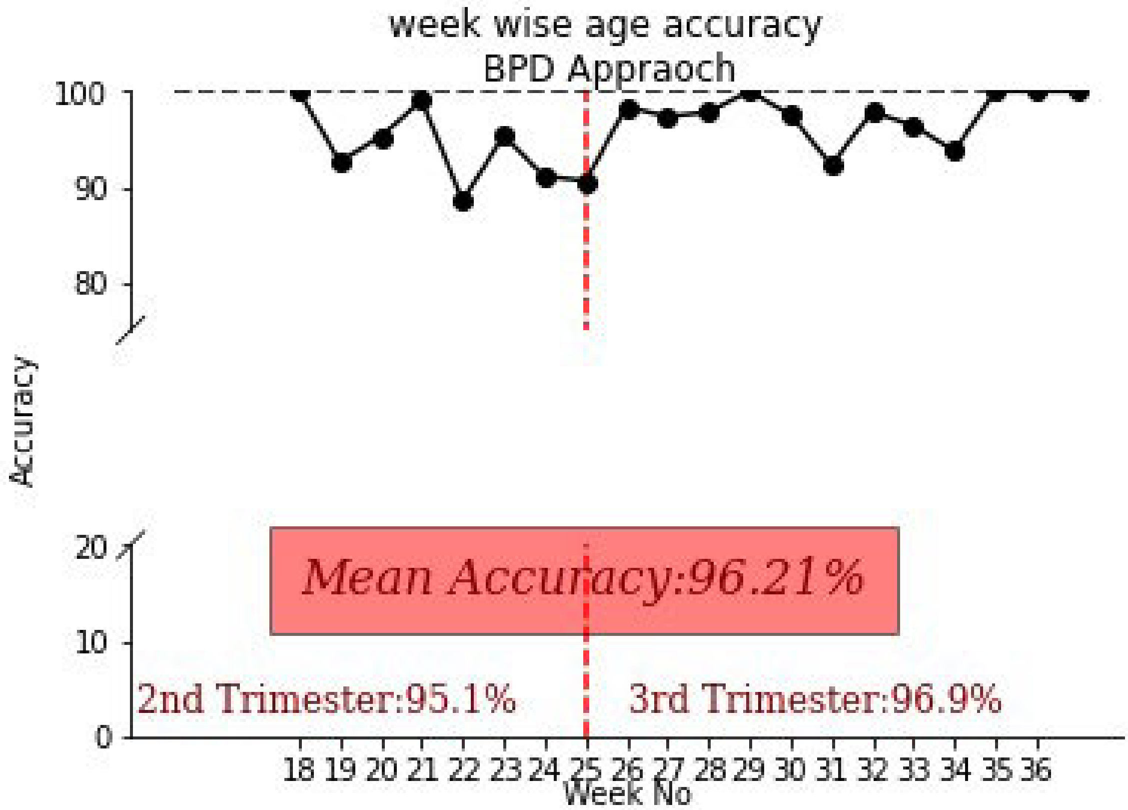

FIGURE 28. Week wise gestational age accuracy with BPD approach and breakdown with semester wise.

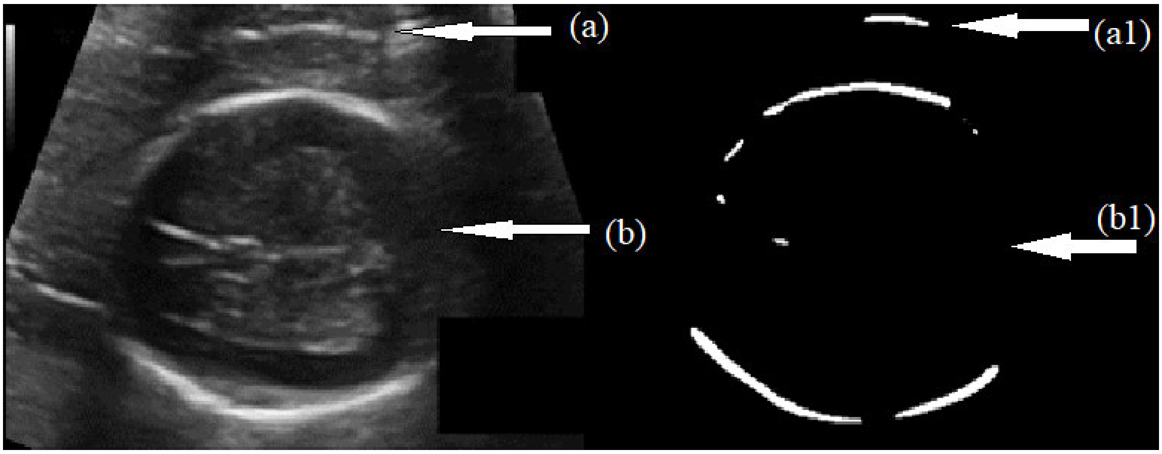

FIGURE 29. Showing curve regions produced while scanning fetal head ultrasound and corresponding binarised segmented image (a) noise on ultrasound image (b) gap between biparietal bones on ultrasound image (a1) noise in binary segmented ultrasound image (b1) gap between biparietal bones in binary segmented ultrasound image.

of the ultrasound video, which generally varies from 15 to 30 minutes of length depending upon the expertise of sonographer [AKUH]. However, it should be noted that during clinical application, this computation time will drop significantly as in addition to automated fetal biometry, system will also be assisting sonographer during scanning process to identify required frames, this in turn will reduce overall duration. Thus in summary, proposed system uses robust machine vision features to reduce the sonographer's interaction with the system, thus reducing the overall procedure time and being independent of the sonographer's skill. The extension of the study can be to automated measurements of femur length and abdomen circumference; for fetal weight estimation.

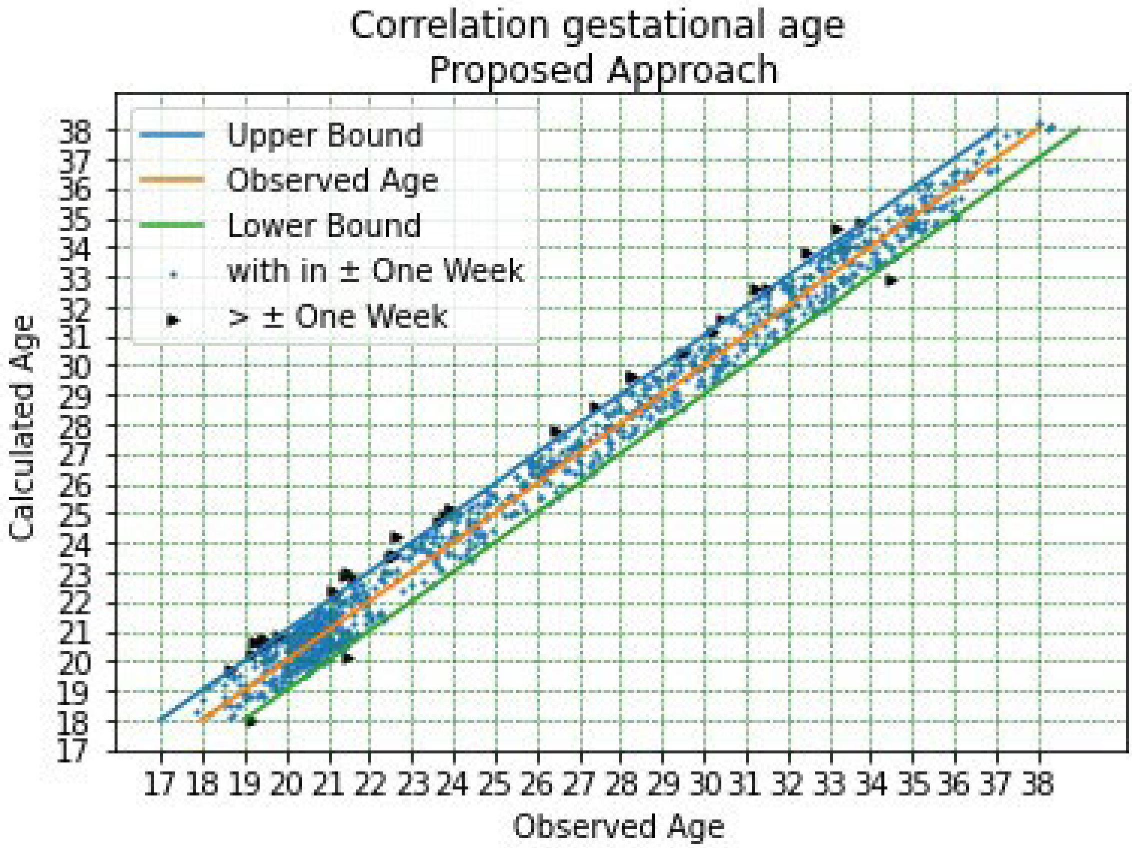

FIGURE 30. Correlation gestational age for observed and calculated using proposed approach with lower and upper bound of one week.

TABLE 8. Trimester wise statistics for acceptance of ultrasound videos with ± one week tolerance.

Parameter used	Trimester	Total Videos	with in ± one week	> ± one week	Acceptance Rate
HC		485	447	38	92.20%
BPD	Second Trimester		461	24	95.10%
Proposed (HC & BPD)			465	20	95.90%
HC		515	481	34	93.40%
BPD	Third Trimester		499	16	96.90%
Proposed (HC + BPD)			500	15	97.10%

ACKNOWLEDGMENT

The authors would like to thank Dr. Noruddin Badruddin, Head of Obstetrics and Gynecology Department, AKUH, and his team's helpful advice during the data acquisition. The authors also appreciate and acknowledge the Open Access Funding by the Publication Fund of the TU Dresden.

REFERENCES

[1] L. Kang, Q.-Q. Wu, L.-J. Sun, F.-Y. Gao, and J.-J. Wang, "Predicting fetal weight by three-dimensional limb volume ultrasound (AVol/TVol) and abdominal circumference," *Chin. Med. J.*, vol. 134, no. 9, pp. 1070–1078, 2021.

[2] E. Dyer and T. Chudleigh, "Peer review of third trimester abdominal circumference measurements," *Ultrasound*, vol. 29, no. 2, pp. 83–91, May 2021.

[3] S. Płotka, T. Włodarczyk, A. Klasa, M. Lipa, A. Sitek, and T. Trzciński, "FetalNet: Multi-task deep learning framework for fetal ultrasound biometric measurements," 2021, *arXiv:2107.06943*.

[4] J. M. J. Arezina, "The accuracy of ultrasound estimation of fetal weight in comparison to birth weight: A systematic review," *Ultrasound*, vol. 26, no. 1, pp. 32–41, Feb. 2018, doi: 10.1177/1742271X17732807.

[5] J. Lanowski, G. Lanowski, J. V. Ehr, M. Jentschke, P. Hillemanns, E. Kuehnle, and I. Staboulidou, "Impact of ultrasound training and experience on accuracy regarding fetal weight estimation at term creative education," *Creative Educ.*, vol. 8, no. 11, pp. 1761–1773, 2017.

[6] S. K. Kristin, C. R. Magner;, W. Carri, and R. Warshak, "Increasing maternal body mass index and the accuracy of sonographic estimation of fetal weight near delivery," *J. Ultrasound Med.*, vol. 33, no. 12, pp. 2173–2179, Dec. 2014.

[7] E. Ashwal, L. Hiersch, N. Melamed, R. Bardin, A. Wiznitzer, and Y. Yogev, "Does the level of amniotic fluid have an effect on the accuracy of sonographic estimated fetal weight at term?" *J. Maternal-Fetal Neonatal Med.*, vol. 28, no. 6, pp. 638–642, Jun. 2014.

[8] N. H. Khan, E. Tegnander, J. M. Dreier, S. Eik-Nes, H. Torp, and G. Kiss, "Automatic detection and measurement of fetal femur length using a portable ultrasound device," in *Proc. IEEE Int. Ultrason. Symp. (IUS)*, Oct. 2015, pp. 1–4, doi: 10.1109/ULTSYM.2015.0486.

[9] M. Corbett, "Sonographer shortages: A day late and a dollar short?" *J. Diagnostic Med. Sonography*, vol. 19, no. 3, pp. 201–202, May 2003.

[10] A. Dempsey and S. Mens, "Sonographer shortages: A day late and a dollar short," *J. Diagnostic Med. Sonography*, vol. 19, no. 3, pp. 205–206, 2003.

[11] A. C. Lee, P. Panchal, L. Folger, H. Whelan, R. Whelan, B. Rosner, H. Blencowe, and J. E. Lawn, "Diagnostic accuracy of neonatal assessment for gestational age determination: A systematic review," *Pediatrics*, vol. 140, no. 6, Dec. 2017, Art. no. e20171423, doi: 10.1542/peds.2017-1423.

[12] M. K. Munos, A. K. Blanc, E. D. Carter, T. P. Eisele, S. Gesuale, J. Katz, T. Marchant, C. K. Stanton, and H. Campbell, "Validation studies for population-based intervention coverage indicators: Design, analysis, and interpretation," *J. Global Health*, vol. 8, no. 2, Dec. 2018, Art. no. 020804, doi: 10.7189/jogh.08.020804.

[13] N. H. Anderson, L. C. Sadler, C. J. D. McKinlay, and L. M. E. McCowan, "INTERGROWTH-21st vs customized birthweight standards for identification of perinatal mortality and morbidity," *Amer. J. Obstetrics Gynecol.*, vol. 214, no. 4, pp. 509.e1–509.e7, Apr. 2016, doi: 10.1016/j.ajog.2015.10.931.

[14] G. M. Buck Louis, J. Grewal, P. S. Albert, A. Sciscione, D. A. Wing, W. A. Grobman, R. B. Newman, R. Wapner, M. E. D'Alton, D. Skupski, M. P. Nageotte, A. C. Ranzini, J. Owen, E. K. Chien, S. Craigo, M. L. Hediger, S. Kim, C. Zhang, and K. L. Grantz, "Racial/ethnic standards for fetal growth: The NICHD fetal growth studies," *Amer. J. Obstetrics Gynecol.*, vol. 213, no. 4, pp. 449.e1–449.e41, Oct. 2015, doi: 10.1016/j.ajog.2015.08.032.

[15] G. E. Hanley and P. A. Janssen, "Ethnicity-specific birthweight distributions improve identification of term newborns at risk for short-term morbidity," *Amer. J. Obstetrics Gynecol.*, vol. 209, no. 5, pp. 428.e1–428.e6, Nov. 2013.

[16] (Jun. 2021). *Head Circumference Calculator*. [Online]. Available: https://www.babymed.com/tools/hc-head-circumference-calculator

[17] R. Savirón-Cornudella, L. M. Esteban, R. Aznar-Gimeno, P. Dieste-Pérez, F. R. Pérez-López, J. M. Campillos, B. Castán-Larraz, G. Sanz, and M. Tajada-Duaso, "Prediction of late-onset small for gestational age and fetal growth restriction by fetal biometry at 35 weeks and impact of ultrasound–delivery interval: Comparison of six fetal growth standards," *J. Clin. Med.*, vol. 10, no. 13, p. 2984, Jul. 2021, doi: 10.3390/jcm10132984.

[18] J. Gardosi, V. Madurasinghe, M. Williams, A. Malik, and A. Francis, "Maternal and fetal risk factors for stillbirth: Population based study," *BMJ*, vol. 346, p. f108, Jan. 2013.

[19] J. Caradeux, R. J. Martinez-Portilla, A. Peguero, A. Sotiriadis, and F. Figueras, "Diagnostic performance of third-trimester ultrasound for the prediction of late-onset fetal growth restriction: A systematic review and meta-analysis," *Amer. J. Obstetrics Gynecol.*, vol. 220, no. 5, pp. 449–459, 2019.

[20] D. W. Skupski, J. Owen, S. Kim, K. M. Fuchs, P. S. Albert, and K. L. Grantz, "Estimating gestational age from ultrasound fetal biometrics," *Obstetrics Gynecol.*, vol. 130, no. 2, pp. 433–441, Aug. 2017.

[21] B. Idowu, A. Azagidi, B. Ibitoye, O. Makinde, and A. Aderibigbe, "Fetal gestational age determination using ultrasound placental thickness," *J. Med. Ultrasound*, vol. 28, no. 1, p. 17, 2020.

[22] F. Yepes-Calderon, F. Wihardja, A. Sloan, J. Kim, M. D. Nelson, and J. G. McComb, "Measuring maximum head circumference within the picture archiving and communication system: A fully automatic approach," *Frontiers Pediatrics*, vol. 9, p. 671, Jul. 2021.

[23] J. Li, Y. Wang, B. Lei, J.-Z. Cheng, J. Qin, T. Wang, S. Li, and D. Ni, "Automatic fetal head circumference measurement in ultrasound using random forest and fast ellipse fitting," *IEEE J. Biomed. Health Informat.*, vol. 22, no. 1, pp. 215–223, Jan. 2018.

[24] T. L. A. van den Heuvel, H. Petros, S. Santini, C. L. de Korte, and B. van Ginneken, "Automated fetal head detection and circumference estimation from free-hand ultrasound sweeps using deep learning in resource-limited countries," *Ultrasound Med. Biol.*, vol. 45, no. 3, pp. 773–785, Mar. 2019.

[25] G. A. Grandjean, G. Hossu, C. Bertholdt, P. Noble, O. Morel, and G. Grangé, "Artificial intelligence assistance for fetal head biometry: Assessment of automated measurement software," *Diagnostic Interventional Imag.*, vol. 99, no. 11, pp. 709–716, Nov. 2018.

[26] M. G. Oghli, A. Shabanzadeh, S. Moradi, N. Sirjani, R. Gerami, P. Ghaderi, M. S. Taheri, I. Shiri, H. Arabi, and H. Zaidi, "Automatic fetal biometry prediction using a novel deep convolutional network architecture," *Phys. Medica*, vol. 88, pp. 127–137, Aug. 2021.

[27] M. C. Fiorentino, S. Moccia, M. Capparuccini, S. Giamberini, and E. Frontoni, "A regression framework to head-circumference delineation from US fetal images," *Comput. Methods Programs Biomed.*, vol. 198, Jan. 2021, Art. no. 105771.

[28] J. C. Prieto, H. Shah, A. J. Rosenbaum, X. Jiang, P. Musonda, J. T. Price, and J. S. Stringer, "An automated framework for image classification and segmentation of fetal ultrasound images for gestational age estimation," *Proc. SPIE*, vol. 11596, Feb. 2021, Art. no. 115961N.

[29] J. Zhang, C. Petitjean, P. Lopez, and S. Ainouz, "Direct estimation of fetal head circumference from ultrasound images based on regression CNN," in *Proc. Medical Imag. With Deep Learn.*, Sep. 2020, pp. 914–922.

[30] D. T. Avalokita, T. Rismonita, A. Handayani, and A. W. Setiawan, "Automatic fetal head circumference measurement in 2D ultrasound images based on optimized fast ellipse fitting," in *Proc. IEEE REGION Conf. (TENCON)*, Nov. 2020, pp. 37–42.

[31] W. F. Farsana and N. Kowsalya, "Automaticfetal head circumference measurement in 2D ultrasound fetal images using histogram of oriented gradient," *Technology*, vol. 11, no. 12, pp. 484–491, 2020.

[32] W. Lu, J. Tan, and R. Floyd, "Automated fetal head detection and measurement in ultrasound images by iterative randomized Hough transform," *Ultrasound Med. Biol.*, vol. 31, no. 7, pp. 929–936, Jul. 2005, doi: 10.1016/j.ultrasmedbio.2005.04.002.

[33] R. V. McManigle, "A boundary fragment model for head segmentation in fetal ultrasound," in *Proc. Challenge US, Biometric Meas. From Fetal Ultrasound Images (ISBI)*, May 2012, pp. 9–11.

[34] A. Ciurte, X. Bresson, O. Cuisenaire, N. Houhou, S. Nedevschi, J.-P. Thiran, and M. B. Cuadra, "Semi-supervised segmentation of ultrasound images based on patch representation and continuous min cut," *PLoS ONE*, vol. 9, no. 7, Jul. 2014, Art. no. e100972, doi: 10.1371/journal.pone.0100972.

[35] A. Foi, M. Maggioni, A. Pepe, S. Rueda, J. A. Noble, A. T. Papageorghiou, and J. Tohka, "Difference of Gaussians revolved along elliptical paths for ultrasound fetal head segmentation," *Computerized Med. Imag. Graph.*, vol. 38, no. 8, pp. 774–784, Dec. 2014, doi: 10.1016/j.compmedimag.2014.09.006.

[36] T. L. A. van den Heuvel, D. de Bruijn, C. L. de Korte, and B. V. Ginneken, "Automated measurement of fetal head circumference using 2D ultrasound images," *PLoS ONE*, vol. 13, no. 8, Aug. 2018, Art. no. e0200412.

[37] K. D. Rahayu, R. Sigit, D. Agata, A. Pambudi, and N. Istiqomah, "Automatic gestational age estimation by femur length using integral projection from fetal ultrasonography," in *Proc. Int. Seminar Appl. Technol. Inf. Commun.*, Sep. 2018, pp. 498–502, doi: 10.1109/ISEMANTIC.2018.8549764.

[38] L. P. Kirthana and N. Muthurasu, "Automatic estimation of fetal head circumference using UNet and Hough transform," in *Proc. IRJET*, vol. 7, Apr. 2020, pp. 2441–2443.

[39] R. Meyer, A. Rottenstreich, M. Zamir, H. Ilan, E. Ram, M. Alcalay, and G. Levin, "Sonographic fetal head circumference and the risk of obstetric anal sphincter injury following vaginal delivery," *Int. Urogynecol. J.*, vol. 31, no. 11, pp. 2285–2290, Nov. 2020.

[40] E. G. M. Kanaga, J. Anitha, and D. S. Juliet, "4D medical image analysis: A systematic study on applications, challenges, and future research directions," in *Advanced Machine Vision Paradigms for Medical Image Analysis*, 2021, pp. 97–130.

[41] B. Goyal, A. Dogra, S. Agrawal, and B. S. Sohi, "Noise issues prevailing in various types of medical images," *Biomed. Pharmacol. J.*, vol. 11, no. 3, pp. 1227–1237, Sep. 2018.

[42] A. Ghorbani, D. Ouyang, A. Abid, B. He, J. H. Chen, R. A. Harrington, D. H. Liang, E. A. Ashley, and J. Y. Zou, "Deep learning interpretation of echocardiograms," *NPJ Digit. Med.*, vol. 3, no. 1, p. 10, Dec. 2020.

[43] M. G. Tolsgaard, M. B. S. Svendsen, J. K. Thybo, O. B. Petersen, K. M. Sundberg, and A. N. Christensen, "Does artificial intelligence for classifying ultrasound imaging generalize between different populations and contexts?" *Ultrasound Obstetrics Gynecol.*, vol. 57, no. 2, pp. 342–343, Feb. 2021.

[44] V. Verfaille, M. C. Haak, E. Pajkrt, A. de Jonge, J. Henrichs, A. Franx, and P. Jellema, "Quality assessment of ultrasonic foetal biometry during the IUGR risk selection (IRIS) trial: A cross sectional study," *Midwifery*, vol. 91, Dec. 2020, Art. no. 102842.

[45] R. Meyer, A. Rottenstreich, M. Shapira, M. Alcalay, E. Ram, Y. Yinon, and G. Levin, "The role of fetal head circumference in the formation of obstetric anal sphincter injuries following vacuum deliveries among primiparous women," *Arch. Gynecol. Obstetrics*, vol. 301, no. 6, pp. 1423–1429, Jun. 2020.

[46] A. Van Binst, N. Kennedy, S. Harland, A. Aziz, and A. Quinton, ''The limitations of access to continuing professional development amongst Australia's rural sonographers and its effect on job satisfaction: A pilot study,'' *Sonography*, vol. 6, no. 2, pp. 43–49, Jun. 2019.

[47] M. Doig, J. Dizon, K. Guerrero, and N. Parange, ''Exploring the availability and impact of antenatal point-of-care ultrasound services in rural and remote communities: A scoping review,'' *Australas. J. Ultrasound Med.*, vol. 22, no. 3, pp. 174–185, Aug. 2019.

[48] A. Østvik, E. Smistad, S. A. Aase, B. O. Haugen, and L. Lovstakken, ''Real-time standard view classification in transthoracic echocardiography using convolutional neural networks,'' *Ultrasound Med. Biol.*, vol. 45, no. 2, pp. 374–384, 2019, doi: 10.1016/j.ultrasmedbio.2018.07.024.

[49] B. Kim, K. C. Kim, Y. Park, J.-Y. Kwon, J. Jang, and J. K. Seo, ''Machine-learning-based automatic identification of fetal abdominal circumference from ultrasound images,'' *Physiolog. Meas.*, vol. 39, no. 10, Oct. 2018, Art. no. 105007.

[50] E. Maini, ''Enhanced direct least square fitting of ellipses,'' *Int. J. Pattern Recognit. Artif. Intel.*, vol. 20, no. 6, p. 939, 2006.

[51] W. Gander, G. H. Golub, and R. Strebel, ''Least-squares fitting of circles and ellipses,'' *BIT Numer. Math.*, vol. 34, no. 4, pp. 558–578, Dec. 1994.

[52] J. D. Shaheen, R. Hershkovitz, S. A. Mastrolia, R. Charach, R. Eshel, D. Tirosh, N. Shaheen, and J. Baron, ''Estimation of fetal weight using Hadlock's formulas: Is head circumference an essential parameter,'' *Eur. J. Obstetrics Gynecol. Reproductive Biol.*, vol. 243, pp. 87–92, Dec. 2019.

[53] J. G. Simonsen, C. Dahlqvist, H. Enquist, C. Nordander, A. Axmon, and I. Arvidsson, ''Assessments of physical workload in sonography tasks using inclinometry, goniometry, and electromyography,'' *Saf. Health At Work*, vol. 9, no. 3, pp. 326–333, Sep. 2018.

[54] R. Hussein, M. B. Gameraddin, B. H. A. Malik, M. Yousef, and Q. Turki, ''Evaluation of gestational age by fetal occipitofrontal diameter in second and third trimesters of pregnancy in Sudanese women,'' *Tropical J. Obstetrics Gynaecol.*, vol. 35, no. 1, pp. 63–67, 2018.

[55] S. Cai, G. Zhang, H. Zhang, and J. Wang, ''Normative linear and volumetric biometric measurements of fetal brain development in magnetic resonance imaging,'' *Child's Nervous Syst.*, vol. 36, no. 12, pp. 2997–3005, Dec. 2020.

[56] R. N. Blue, E. M. Beddow, M. Savabi, R. V. Katukuri, and R. C. Chao, ''Comparing the Hadlock fetal growth standard to the *eunice kennedy Shriver* National Institute of Child Health and Human Development racial/ethnic standard for the prediction of neonatal morbidity and small for gestational age,'' *Amer. J. Obstetrics Gynecol.*, vol. 219, no. 5, pp. 474.e1–474.e12, 2018, doi: 10.1016/j.ajog.2018.08.011.

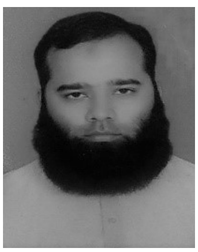

KHALID RASHEED received the bachelor's degree from Karachi University, Pakistan, and the M.S. degree in computer science from SZABIST, Karachi, Pakistan, where he is currently pursuing the Ph.D. degree in computer science. He has gained academic and industrial experience in his professional career. His research interests include machine learning, computer vision, image processing, data sciences, and cyber security.

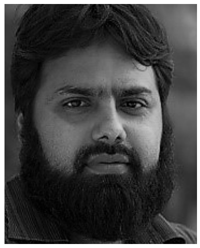

FARAZ JUNEJO received the Ph.D. degree in mechatronics engineering from Loughborough University, U.K. He is currently the Head of the Department of Mechatronics Engineering, SZABIST. He has more than ten years of research experience. His research interests include smart industries, computer/machine vision, digital image and signal processing, and artificial intelligence.

AYESHA MALIK received the M.B.B.S. and F.C.P.S. degrees. She is one of the top certified Gynecologist in Karachi. Currently, she is practicing at Aga Khan University Hospital. She has advanced medical expertise in gynecology and is providing the following services: diagnosing hormonal imbalance problems in girls, infertility, PCOS, menopause in elderly women, pregnancy issues, treating and diagnosing STIs, Pelvic diseases, mood changes, urinal issues in women, reproductive health, sexual dysfunction, pregnancy related tumors and cancer development in reproductive tracts, contraception, sterilization, miscarriage, and other pregnancy issues.

MUHAMMAD SAQIB received the B.S. degree in biomedical engineering from the Sir Syed University of Engineering and Technology, Pakistan, and the M.S. degree in electronic engineering from Hamdard University, Karachi, Pakistan. He is currently pursuing the joint Ph.D. degree in biomedical engineering with Fraunhofer IKTS, Dresden, Germany, and TU Dresden, Dresden.

He has gained academic and industrial experience in his professional career. He has two patents and several peer-reviewed conferences and journal publications. He received the HEC Pakistan/DAAD Germany Scholarship for his Ph.D. studies. His research interests include the stent degradation, bioinstrumentation, biomaterials, biometrics, biomechanics, and corrosion.